Year: 2018

JNK1 induces hedgehog signaling from stellate cells to accelerate liver regeneration in mice

Langiewicz, Magda ; Graf, Rolf ; Humar, Bostjan ; Clavien, Pierre A

Abstract: Background Aims To improve outcomes of two-staged hepatectomies for large/multiple liver tumors, portal vein ligation (PVL) has been combined with parenchymal transection (associating liver partition and portal vein ligation for staged hepatectomy [coined ALPPS]) to greatly accelerate liver regeneration. In a novel ALPPS mouse model, we have reported paracrine Indian hedgehog (IHH) signaling from stellate cells as an early contributor to augmented regeneration. Here, we sought to identify upstream regulators of IHH. Methods ALPPS in mice was compared against PVL and additional control surgeries. Potential IHH regulators were identified through in silico mining of transcriptomic data. c-Jun N-terminal kinase (JNK1 [Mapk8]) activity was reduced through SP600125 to evaluate its effects on IHH signaling. Recombinant IHH was injected after JNK1 diminution to substantiate their relationship during accelerated liver regeneration. Results Transcriptomic analysis linked Ihh to Mapk8. JNK1 upregulation after ALPPS was validated and preceded the IHH peak. On immunofluorescence, JNK1 and IHH co-localized in alpha-smooth muscle actin-positive non-parenchymal cells. Inhibition of JNK1 prior to ALPPS surgery reduced liver weight gain to PVL levels and was accompanied by downregulation of hepatocellular proliferation and the IHH-GLI1-CCND1 axis. In JNK1-inhibited mice, recombinant IHH restored ALPPS-like acceleration of regeneration and re-elevated JNK1 activity, suggesting the presence of a positive IHH-JNK1 feedback loop. Conclusions JNK1-mediated induction of IHH paracrine signaling from hepatic stellate cells is essential for accelerated regeneration of parenchymal mass. The JNK1-IHH axis is a mechanism unique to ALPPS surgery and may point to therapeutic alternatives for patients with insufficient regenerative capacity. Lay summary Associating liver partition and portal vein ligation for staged hepatectomy (so called ALPPS), is a new two-staged approach to hepatectomy, which induces an unprecedented acceleration of liver regeneration, enabling treatment of patients with liver tumors that would otherwise be considered unresectable. Herein, we demonstrate that JNK1-IHH signaling from stellate cells is a key mechanism underlying the regenerative acceleration that is induced by ALPPS.

DOI: https://doi.org/10.1016/j.jhep.2018.04.017

Originally published at:
Langiewicz, Magda; Graf, Rolf; Humar, Bostjan; Clavien, Pierre A (2018). JNK1 induces hedgehog signaling from stellate cells to accelerate liver regeneration in mice. Journal of Hepatology, 69(3):666-675.
DOI: https://doi.org/10.1016/j.jhep.2018.04.017

JNK1 induces IHH signaling from stellate cells to accelerate liver regeneration after ligation and transection in mice

Short title: JNK1 accelerates liver regeneration via IHH

Authors: Magda Langiewicz[1], Rolf Graf[1], Bostjan Humar[1*], and Pierre A. Clavien[1*].

*shared senior authorship

Affiliations: [1]Laboratory of the Swiss Hepato-Pancreato-Biliary (HPB) and Transplantation Center, Department of Surgery, University Hospital Zurich, Raemistrasse 100, Zurich, CH-8091, Switzerland.

Grant support: This study was funded by the Clinical Research Priority Program (CRPP) from the University of Zurich "non-resectable liver tumors – from palliation to cure" and the Swiss National Science Foundation (S-87002-09-01).

Abbreviations: ALPPS: Associating Liver Partition and Portal Vein Ligation Surgery, FLR: functional liver remnant, HSC: hepatic stellate cells, Ihh: Indian hedgehog, JNK1: c-Jun-N-terminal kinase, pH3: phosphohistone 3; PVL: Portal Vein Ligation, SFSS: small-for-size-syndrome, PH: partial hepatectomy

Corresponding author: Pierre-Alain Clavien, Department of Surgery & Transplantation, University Hospital Zurich, Raemistrasse 100, CH-8091 Zurich, Phone: +41 44 255 3300, email: clavien@access.uzh.ch

Disclosures and conflict of interest statement: All authors contributing to this manuscript declare that they have nothing to disclose. They do not have a conflict of interest with respect to this manuscript.

Transcript Profiling: ENA PRJEB15593

Authors contributions: Experimental design: ML, BH. Data acquisition and analyses: ML, BH. Data interpretation: BH, ML, RG. Study concept and design: BH. Manuscript writing & critical revision: ML, BH, PAC. Funding: PAC, BH, RG. All authors approved the final version.

Electronic word count: 5849

References: 46

Figures: 6

Email addresses of authors: magda.langiewicz@usz.ch, rolf.graf@usz.ch, bostjan.humar@usz.ch, clavien@access.uzh.ch

Keywords: compensatory hypertrophy; small-for-size syndrome; future liver remnant.

Abstract

Background & Aims: To improve outcomes of two-staged hepatectomies for large/multiple liver tumors, portal vein ligation (PVL) has been combined with parenchymal transection (coined ALPPS; *A*ssociated *L*iver *P*artition and *P*ortal vein ligation for *S*taged hepatectomy) to greatly accelerate liver regeneration. In a novel ALPPS mouse model, we have reported paracrine Indian hedgehog (IHH) signaling from stellate cells as an early contributor to augmented regeneration. Here, we sought to identify upstream regulators of IHH.

Methods: ALPPS in mice was compared against PVL and additional control surgeries. Potential IHH regulators were identified through *in silico* mining of transcriptomic data. JNK1 activity was reduced through SP600125 to evaluate its effects on IHH signaling. Recombinant IHH was injected after JNK diminution to substantiate their relationship during accelerated liver regeneration.

Results: Mining linked *Ihh* to *Mapk8*. JNK1 upregulation after ALPPS was validated and preceded the IHH peak. On immunofluorescence, JNK1 and IHH co-localized in ASMA-positive non-parenchymal cells. Inhibition of JNK1 prior to ALPPS surgery reduced liver weight gain to PVL levels and was accompanied by downregulation of hepatocellular proliferation and the IHH-GLI1-CCND1 axis. In JNK1-inhibited mice, recombinant IHH restored ALPPS-like acceleration of regeneration and re-elevated JNK1 activity, suggesting the presence of a positive IHH-JNK1 feedback loop.

Conclusions: JNK1-mediated induction of IHH paracrine signaling from HSCs is essential for accelerated regeneration of parenchymal mass. The JNK1-IHH axis is a mechanism unique to ALPPS surgery and may point to therapeutic alternatives for patients with insufficient regenerative capacity.

Lay Summary: ALPPS, a novel two-staged hepatectomy, induces an unprecedented acceleration of liver regeneration to enable treatment of unresectable liver tumors. Here, we demonstrate JNK1-IHH signaling as a mechanism underlying the regenerative acceleration induced by ALPPS.

Introduction

The unique ability of mammalian liver to regain mass after tissue loss has revolutionized the treatment and cure of many patients with liver tumors. However, there are limitations to effective regeneration, as hepatic failure may develop after extensive liver resection. This entity, known as the small-for-size syndrome (SFSS), results from an insufficient functional volume of the liver remnant and remains the most frequent cause of death due to liver surgery.[1, 2] Two-staged hepatectomies were introduced to reduce the SFSS risk. Typically, the portal vein draining the part of the liver containing the tumor is occluded (step 1), causing growth of the contralateral liver part (defined as the future remnant liver (FRL)); when the FRL has gained sufficient functional volume, step 2 (resection of the diseased part) is performed.[2, 3] Nevertheless, in some cases regeneration is still insufficient, or the considerable time period between step 1 and 2 allows for further progression of the disease.[4, 5] To additionally reduce the risk of SFSS in patients with large or multiple liver tumors, ALPPS (*A*ssociated *L*iver *P*artition and *P*ortal vein ligation for *S*taged hepatectomy: the combination of portal vein ligation with parenchymal transection) has been showcased as a procedure that induces accelerated liver regeneration and greatly reduces the interval between steps, allowing treatment of patients otherwise deemed as unresectable.[6, 7] This procedure, introduced about five years ago, has gained sustained acceptance with more than 1000 cases included in an international registry (http://www.alpps.net/?q=registry).

Although there have been several clinical studies evaluating ALPPS in patients, reports on the molecular mechanisms underlying the regenerative acceleration following ALPPS-step 1 remain scarce. Several components known to be necessary for liver regeneration after partial hepatectomy have likewise been associated with accelerated regeneration. In rodent models, IL-6 and TNFα - established mediators of liver regeneration - have been found upregulated in ALPPS at the mRNA and protein level. Similarly, protein expression of STAT3, RELA, and YAP1 – known transcription factors in the regenerating liver - were elevated after ALPPS step 1.[8, 9] Furthermore, hypoxia has recently been shown to be an important driver of normal regeneration through HIF2α, with preliminary studies pointing to the importance of hypoxia also in ALPPS.[10, 11] In human ALPPS

tissues, IL-6 and TNFα have been validated on the mRNA level.[12] However, none of these molecules seems to be unique to the ALPPS-induced acceleration of regeneration.

We have developed a mouse model of ALPPS and documented the release of serum factors that can accelerate regeneration in mice following portal vein ligation (PVL) only to levels seen after the complete ALPPS-step 1 procedure.[12] These findings suggest that humoral factors must play essential roles in the early instigation of accelerated regeneration. With this mouse model, we established that the secretion of Indian Hedgehog (IHH) from hepatic stellate cells (HSCs) was necessary for the early activation and progression of accelerated regeneration.[13] Although hedgehog signaling has previously been reported to be required for regeneration after hepatectomy, the early elevations in serum IHH were unique to ALPPS, and not observed following hepatectomy or other surgeries.[13]

Hedgehog activity is barely detectable in healthy adult liver. Upon hepatectomy, however, hepatocytes begin to proliferate and HSCs undergo differentiation into myofibroblastic and fibrogenic states.[14, 15] Furthermore, there is increasing evidence that morphogenic signals - such as the hedgehog pathway - are mediators of the myofibroblastic HSC switch. When blocking or knocking out *Smo*, the receptor for hedgehog ligands, HSCs do not acquire myofibroblastic traits, and subsequent hepatocyte regeneration is inhibited.[16, 17, 18]

Given the specific secretion of IHH after ALPPS, this study sought to identify upstream regulators of the ligand as to establish the role of IHH in ALPPS. On the other hand, expanding on the networks that act to accelerate regeneration after ALPPS may provide insight into new therapeutics for the pharmacological promotion of regeneration in clinical settings.

Materials and Methods

Animals

All animal experiments were performed in accordance with Swiss Federal Animal Regulations and approved by the Veterinary Office of Zurich. Male C57Bl/6 mice (Envigo, Horst, NL) aged 10-12 weeks kept on a 12-hour day/night cycle with free access to food and water were used.

Animal surgery and treatment

To mimic human ALPPS surgery in mice, 90% PVL was performed leaving a 10% functional remnant consisting of the left and a part of the right middle lobe. Then, a partial 80% transection was done through the middle lobe along the demarcation line of the occluded/non-occluded parenchyme. The left lateral lobe (LLL, 25% of liver volume) was also resected to simulate the cleaning of the liver from smaller tumors as often done in human ALPPS. Details on isoflurane anesthesia, buprenorphine analgesia, ALPPS procedures, and the control operations (90% PVL, 80% transection, and sham laparotomy) have been described.[12, 13] After surgery, animals were allowed to recover on a warming pad in a separate cage until completely conscious. Animals were weighed before surgery and at sacrifice, where weight of resected and remnant liver was recorded. Tissue was formalin fixed or snap frozen, while plasma was stored at -80°C for analysis.

SP600125 (0.016mg/gram BW, InVivoGen, tlrl-sp60 Toulouse, FR), a specific JNK inhibitor, or DMSO in oil was injected I.P. one hour before operation. Recombinant Ihh (200 ng/kg, 160µl final volume; R&D, 1705-HH-025/CF Minneapolis, MN) or PBS was injected into the vena cava right after operation. Ihh antibody (4ug/kg, 160µl final volume; R&D MAB8048) or PBS was injected via tail vein one hour before operation.

Liver regeneration

Liver regeneration was assessed by the percentage of functional-liver-remnant-to-body weight ratio (FLR/BW) derived from six animals per group and time point.

In-silico analysis

RNA sequencing raw data of the accession number PRJEB15593 in the European Nucleotide Archive (ENA) was used for in-silico analysis via the online String Database (string-db.org).

Protein analysis

Western blotting was performed as described.[19] Antibodies are listed in Supplementary Table 2. NE-PER Nuclear and Cytoplasmic Extraction reagents (Thermo Fisher Scientific, Waltham, MA, PK207589) were used to isolate subcellular fractions, with their separation ascertained through β-tubulin (cytoplasmic) and lamin B1 (nuclear) blotting. IHH protein levels were measured by ELISA (mouse IHH: Cusabio, CSB-E16517m). Immunoblots are provided in Supplementary File Immunoblots.

Statistical Analysis.

Data are expressed as mean ±SD. Differences between groups (n=6/group unless for expression profiling with n=3/group and for histological counting with n=5/group) were determined using unpaired, two-tailed t tests assuming unequal variance via GraphPad Prism v4.0 (GraphPad, San Diego CA), with significance set at $P<0.05$. Analyses were performed in a blinded way.

Results

Early upregulation of JNK1 in accelerated liver regeneration

To identify potential upstream regulators of the IHH pathway in accelerated liver regeneration we conducted an *in-silico* analysis of our RNA sequencing data sets derived from livers at early times after ALPPS, PVL, transection, or sham surgery.[13] Genes that discriminated ALPPS liver from other surgeries were included. Using string.db.org, *Mapk8* was text-mined to be linked to *Ihh* and *Ccnd1* of the hedgehog pathway (Fig 1A). Our RNA seq data suggested *Mapk8* upregulation at early times after ALPPS, which we confirmed by qPCR in a new set of animals subjected to the different surgeries (Figure 1B). The deregulation of JNK1 was further confirmed on the protein level. pJNK1, the active form of JNK phosphorylated on Thr183 and Tyr185, was upregulated as early as 1 hour after ALPPS (Fig 1C). Therefore, JNK1 activation through ALPPS surgery precedes the serum IHH peak that we have previously observed at 4h post operation.[13] From these findings, we hypothesized that JNK1 plays a part in accelerated liver regeneration as a potential instigator of IHH signaling.

Ihh and JNK1 are present in activated non-parenchymal cells

To establish an association between JNK1 and IHH signaling, we stained liver sections 4h after operation (ALPPS, PVL, transection, and sham) for IHH, ASMA (a marker of activated hepatic stellate cells), [20, 21] and pJNK1. Non-parenchymal cells were positive for all the three proteins across samples (Supplementary Fig 1), suggesting pJNK1 and IHH may interact in stellate cells to accelerate regeneration. To assess localization of IHH and pJNK1 in activated hepatic stellate cells, we applied immunofluorescence (Fig 2A, Supplementary Fig 2) to paraffin-embedded liver sections after operation. pJNK1 co-localized with both αSMA and IHH, indicating their simultaneous presence in activated stellate cells.

JNK1 is thought to preferentially act in nuclei when phosphorylated.[22, 23] To substantiate an JNK-IHH association, we prepared cytosolic and nuclear fractions from liver at 4h and 24h post surgery and assessed protein levels of pJNK1, the IHH downstream effector and transcription factor

GLI1, and its proliferative target CCND1.[13] Indeed, the nuclear increases in pJNK were paralleled by increases in GLI1, while nuclear levels of total JNK1 and GLI2 remained unchanged (Supplementary Fig 3). CCND1 was significantly elevated at 24h in nuclear fractions (Figure 2C), fitting its delayed induction seen on immunoblots 8h after ALPPS as previously reported.[13] On the other hand, a non-significant elevation in CCND1-positive hepatocyte nuclei was noted on immunohistochemistry at 4h post ALPPS, and was accompanied with increases in proliferative marker (Ki67, pH3) counts. Likewise, the elevated nuclear CCND1 positivity correlated with Ki67/pH3 increases at 24h post ALPPS (Figure 2C, Supplementary Fig 4).

These findings associate JNK1 activation with both the induction of IHH signaling and the promotion of proliferation following ALPPS. Therefore, JNK1 may foster regeneration in ALPPS by causing release of IHH from stellate cells to induce paracrine proliferation of hepatocytes via GLI1-CCND1.[13, 22, 24, 25, 26]

Reduction of JNK1 activity in ALPPS-treated mice abolishes regenerative acceleration

If the elevated activity of JNK1 after ALPPS is promoting acceleration of regeneration, inhibiting JNK should reduce the ALPPS effects. To decrease JNK1 activity, we chose SP600125, a specific JNK inhibitor that has been widely used in liver regeneration studies due to its specificity and ease of application.[27, 28] SP600125 was injected 1h prior to ALPPS surgery, and the assessment of pJNK1 levels in nuclear fractions confirmed a partial inhibition of the protein, with pJNK1 declining to levels seen in mice 4h after PVL (Fig 3A, Supplementary Fig 5).

DMSO vehicle injections had no significant impact on body and liver weight after ALPPS, although DMSO seemed to reduce the ALPPS effects slightly. In contrast, SP600125 significantly reduced the FLR/BW down to levels seen after PVL (Figure 3B). Congruent changes were observed for the proliferative markers Ki67 and pH3 in SP600125-treated animals (Figure 3C, Supplementary Figure 6). We conclude that partial JNK inhibition prior to ALPPS surgery reduces the regenerative

speed to levels comparable to those after PVL. Therefore, JNK1 is an important instigator of the ALPPS-specific acceleration of liver regeneration.

The inhibition of JNK1 downregulates the IHH-GLI1-CCND1 axis in hedgehog signaling

To determine whether JNK1 may act through IHH signaling, we assessed the IHH pathway components in ALPPS mice treated with SP6100125 or control DMSO injection.

Following ALPPS, IHH protein levels peak in serum at 4h with little changes in the liver, consistent with the secretion of the ligand from stellate cells. The increases in serum IHH then promote GLI1 nuclear translocation, downregulation of the hedgehog inhibitor HHIP, and CCND1 upregulation from 4h onwards after ALPPS.[13] Treatment with SP600125 reduced both serum and hepatic levels of IHH 4h post ALPPS (Figure 4A), suggesting JNK1 inhibits production and/or release of the hedgehog ligand. Consistent with IHH downregulation, *Gli1* expression was decreased at 4h and 24h (Figure 4B), while *Hhip* expression was increased by SP600125 treatment at 4h after ALPPS (Figure 4C). Likewise, GLI1 protein and its target CCND1 were downregulated in nuclear fractions of ALPPS liver at 4h and 24h compared to vehicle controls (Figure 4C). Immunohistochemistry confirmed the reductions in nuclear GLI1 and CCND1 (Figure 4E-F, Supplementary Figure 9) with SP600125 treatment. No significant expression changes were observed for *Ptch1, Smo, Gli2* (Supplementary Figure 7) and nuclear GLI2 (Supplementary Figure 8), all molecules the expression of which does not change following IHH stimulation in ALPPS.[13] These findings identify IHH signaling as a potential mediator of JNK1's ability to accelerate regeneration in ALPPS.

Recombinant IHH rescues ALPPS-induced regeneration after JNK inhibition

If JNK1 is promoting its accelerating effects through IHH signaling, restoring IHH levels in SP600125-treated liver should re-accelerate the regenerative response after ALPPS surgery.

Mice were pretreated with SP600125, ALPPS-operated, injected with recombinant ligand (rIHH), and compared to vehicle (DMSO & PBS)-treated ALPPS controls. When assessing body weight after all treatments, no differences were observed between the groups. In contrast, the FLR/BW was

significantly elevated after ALPPS+SP6+rIHH compared to ALPPS+SP6 (Figure 5A). Notably, DMSO/PBS injection on its own seemed to have some negative impact on ALPPS-regeneration. Nonetheless, liver weight was statistically similar for the ALPPS+DMSO+PBS and the ALPPS+SP6+rIHH groups (Figure 5A). Likewise, congruent changes were observed for the proliferative markers Ki67 and pH3 (Figure 5B, Supplementary Figure 10). Therefore, rIHH can compensate for the inhibition of JNK1 during ALPPS-associated regeneration.

Recombinant IHH re-instates hedgehog signaling and promotes JNK1 activity in SP600125-treated ALPPS liver

To further elucidate the relationship between JNK1 and IHH in ALPPS, we evaluated the levels of the individual pathway components. In SP600125-ALPPS-treated mice, rIHH increased *Gli1* and decreased *Hhip* expression (Figure 6A), as well as promoted nuclear GLI1 and CCND1 on immunoblots and immunochemistry (Figure 6B-D, Supplementary Figure 11). Again, *Ptch*, *Smo*, *Gli2* (Supplementary Figure 12), and GLI2 (Supplementary Figure 13) were not significantly affected. Intriguingly, when assessing JNK1, rIHH also increased the levels of nuclear JNK1 (Supplementary Figure 14) and of nuclear pJNK1 on both immunoblots (Figure 6E) and immunohistochemistry (Supplementary Figure 15). Therefore, IHH can increase the activity of JNK1 in ALPPS liver with partially inhibited JNK1, suggesting the presence of a positive feedback loop between JNK1 and IHH. Altogether, these findings establish IHH as a downstream effector of JNK1 in the acceleration of regeneration after ALPPS surgery.

Discussion

Liver regeneration is a complex molecular response unique in its ability to restore full function to the organ.[29] Many pathways have been identified to participate, such as signaling through the hedgehog pathway.[18,28] Nevertheless, liver regeneration does not occur in all patient scenarios, as liver failure ensues if the loss of functional tissue is too extensive.[4] With the introduction of ALPPS, the regenerative capacity has been extended and is expected to improve outcomes of two-staged hepatectomies in patients with marginal qualifications for resection. The unprecedented effect of ALPPS on liver recovery has provoked strong interest in the mechanisms underlying the acceleration of liver regeneration.

Here, we demonstrate a hitherto undescribed interaction between JNK1 and IHH in stellate cells that acts to instigate accelerated liver regeneration early after ALPPS step 1 surgery. More specifically, we demonstrate that (i) JNK1 activation is associated with liver weight gain and precedes the upregulation of IHH-GLI1-CCND1 signaling, (ii) partial inhibition of JNK1 reduces the rate of regeneration to that seen after PVL alone, along with congruent decreases in the IHH-GLI1-CCND1 axis, and that (iii) recombinant IHH is sufficient to restore ALPPS regeneration in JNK1-inhibited mice.

The alterations we observed following ALPPS, SP600125, and rIHH treatments were consistently reflected in GLI1-CCND1 nuclear levels and were strongly correlated with changes in proliferative markers as well as liver weight changes. On the other hand, molecules of the hedgehog pathway that were not affected through IHH (i.e. Ptch, Smo, GLI2) were also not altered through JNK1 manipulation. Moreover, the changes in these hedgehog components were examined via PCR, Western blots as well as immunohistochemical approaches. Therefore, we can reliably conclude that JNK1 initiates the IHH-GLI1-CCND1 axis in accelerated regeneration.

As a limitation to this study, pharmaceutical inhibition was employed to inhibit JNK1 activity during our ALPPS experiments. Genetic knockout models may provide more clear-cut evidence; however, we decided for a pharmacological approach to reduce rather than block JNK activity, given the presence of low levels of pJNK1 also after PVL, the main ALPPS control surgery. Knockdown

strategies may be an alternative, however SP600125 has been widely used in liver research including regeneration studies, [22, 23, 26, 28, 32] rendering our study comparable to existing work on hepatic JNK.

JNK1's role after partial hepatectomy has been revealed by the observation that its inhibition blocks hepatocyte proliferation and liver regeneration.[18, 28, 30] JNK1 is activated within one hour after partial hepatectomy, leading to AP-1 activation, the promotion of cyclin D1 expression, and hepatocellular G0-G1 transition.[22, 30, 31] Interestingly, through studies in fibrosis, JNK1 was found to be involved in HSC activation, where it promotes ASMA expression and HSC proliferation.[22, 32] The morphogenic hedgehog network likewise is recognized to be essential to liver regeneration and to promote expansion of activated HSCs.[13, 15, 18, 33] However, whether JNK1 interacts with the Hedgehog pathway after partial hepatectomy is unknown.

In analogy to regeneration after partial hepatectomy, we observed JNK1 upregulation one hour after ALPPS. Furthermore, JNK1 localized to activated HSCs. The co-localization of IHH and JNK1 in activated HSCs suggested a novel link between these two molecules, which we could demonstrate through SP600125 and recombinant IHH. Indeed, studies in skin cancer have revealed a link between JNK1 and the hedgehog pathway; there, JUN (the canonical JNK1 target) required synergistic interaction with GLI1 for full activation of downstream molecules.[34] Therefore, complex interactions appear to exist between JNK1 and hedgehog signaling.

Unlike after partial hepatectomy, ALPPS did not increase the number of ASMA-positive cells, suggesting JNK1 activity does not promote HSC activation in these settings. While JNK1 clearly promotes regeneration after hepatectomy and ALPPS, the associated mechanisms seem to differ in some aspects. In ALPPS, the interaction between JNK1 and IHH is key in instigating accelerated regeneration. The extent to which IHH participates in regeneration after hepatectomy is unknown; however, the early, strong IHH secretion is unique after ALPPS, as plasma IHH increases occur at much later times and only at modest levels after resection.[13, 18] On the other hand, we observed a statistically significant elevation of serum SHH at 4h after partial hepatectomy relative to ALPPS [13], suggesting SHH rather than IHH may be the hedgehog ligand relevant after resection. However, whether JNK1 is interacting with SHH after hepatectomy remains unknown. In mice, hepatectomy

leads to little parenchymal injury, whereas in ALPPS, liver injury through parenchymal transection is preceded by ligation, which on its own induces regeneration through mechanisms that are ill-defined. Therefore, the divergent nature of the initial regenerative stimuli may underlie the timing and the set of interacting proteins/pathways that define the speed of regeneration after a given surgery.

In this regard, an intriguing observation is that recombinant IHH not only restored accelerated regeneration in SP600125-treated mice, but in parallel increased the activity of the partially inhibited JNK1. These findings imply IHH enhances JNK1 activities in retrograde to promote its own secretion. While further evidence is required to establish such mechanisms, a positive feedback loop between JNK1 and IHH would provide an attractive explanation for the enhanced IHH secretion and the regenerative acceleration unique to ALPPS.

Interestingly, both JNK and Hedgehog have prominent roles in the handling of liver injury. JNK is most notably activated by TNF-alpha, a cytokine involved in the pathophysiology of many types of liver injury, including viral hepatitis, alcoholic liver disease, and ischemia-reperfusion injury. Activated JNK phosphorylates its targets (c-Jun, ATF-2, and JunD), and these transcription factors then activate genes that are involved in the regulation of inflammation, proliferation, and cell death. In the past few years, the use of JNK inhibitors has led to the understanding that the duration of JNK activation is critical for its pro-apoptotic effects in injury.[35] For example, *Gunawan et al* showed that transient blockade of JNK activity through SP600125 was able to rescue mice from acetaminophen-induced liver injury.[36] Similarly, the Hedgehog pathway has been identified to play a role in liver repair such as in regeneration and acute liver injury. In fibrogenic repair, production of Hedgehog ligands increases to permit ligand-receptor interaction and activation of the Hedgehog signaling pathway, which is thought to be vital for the reconstitution of normal liver architecture.[37] In other tissues such as skin, reduced SHH production has been associated with the delayed healing seen in mice with diabetes, a condition closely related to liver disease.[38] Therefore, transient activation of JNK and Hedgehog pathways are important physiological processes fostering the repair of injured liver tissue.

Chronic activation of JNK1, however, has been associated with the development and progression of hepatocellular carcinoma (HCC).[39] Consistent JNK1 activity has been reported to predict a bad outcome in HCC, an aspect that perhaps relates to JNK1 activation secondary to chronic liver injury, an accepted cause of HCC. Although the pro-apoptotic function of JNK1 has been related to anti-cancerous actions,[40] recent evidence indicates a more complex situation, as JNK1 may directly promote the repair of DNA breaks.[39] These observations suggest a disturbed balance between the removal or repair of damaged hepatocytes that underlies JNK1's association with a bad HCC outcome.[39] Indeed, a dual role of JNK1 in HCC has been postulated through animal models, where either its loss or its overactivation contribute to the development of malignancy.[22] Similarly, chronic hedgehog signaling has been linked to HCC. High levels of hedgehog components in HCC seem to maintain the proliferation of cancer stem cells, thereby contributing to HCC progression.[41] Likewise, liver diseases associated with chronic injury and an elevated HCC risk (i.e. nonalcoholic fatty liver disease) are accompanied by a chronic overactivation of the hedgehog pathway.[42] On the other hand, JNK1 and hedgehog activities remain associated with the successful healing of tissue injury, consistent with the view that transient activity of these molecules may be beneficial for the liver.[16, 18, 28, 31, 38, 43]

The first cases of ALPPS occurred in patients in Germany where the technique to induce accelerated regeneration of the liver was discovered by chance.[6, 7] By combination of portal vein ligation and transection, extensive tumor resection was performed and patient recovery occurred in record time.[44, 45, 46] The understanding of ALPPS-triggered processes is in its infancy; however, underlying mechanisms begin to emerge, with the JNK1-IHH axis a first example of ALPPS-specific molecular events that can be associated with the unprecedented regenerative acceleration. Short-term activation of JNK1 and IHH might be of use in the clinic. Not every patient requiring ALPPS may qualify for this major surgery; for example, highly morbid patients that may tolerate PVL, but not the more invasive ALPPS, may benefit from a JNK1-IHH-based promotion of regeneration. Although the oncological risks associated with long-term activation will not vanish, the prevention of imminent death due to liver failure may justify the use of compounds activating the JNK1-IHH pathway. Understanding the extent to which the JNK1 and IHH signals can be stimulated may open the

opportunity for pharmacological administration to encourage regeneration in at-risk-patients, eventually expanding the boundaries of success in the treatment of liver disease one step further.

Acknowledgements

We would like to Udo Ungethüm, Ursula Süss, and Pia Fuchs for excellent technical assistance.

References

1. Clavien PA, Oberkofler C, Raptis DA, Lehmann K, Rickenbacher A, El-Badry A. What is critical for liver surgery and partial liver transplantation: size or quality? Hepatology 2010;52:712-729.
2. Clavien PA, Petrowsky H, DeOliveira M, Graf R. Strategies for safer liver surgery and partial liver transplantation. N Engl J Med 2007;356:1545-1559.
3. Jaeck D, Oussoultzoglou E, Rosso E, Greget M, Weber JC, Bachellier P. A two-stage hepatectomy procedure combined with portal vein embolization to achieve curative resection for initially unresectable multiple and bilobar colorectal liver metastases. Ann Surg 2004;240:1037-1049.
4. Donati M, Stavrou GA, Oldhafer KJ. Current position of ALPPS in the surgical landscape of CRLM treatment proposals. World J Gastroenterol 2013;19:6548-6554.
5. Schadde E, Ardiles V, Slankamenac K, Tschuor C, Sergeant G, Amacker N, et al. ALPPS offers a better chance of complete resection in patients with primarily unresectable liver tumors compared with conventional-staged hepatectomies: results of a multicenter analysis. World J Gastroenterol 2014;38:1510-1519.
6. de Santibañes E, Clavien PA. Playing Play-Doh to prevent postoperative liver failure: the "ALPPS" approach. Ann Surg 2012;255:415-417.
7. Schnitzbauer AA, Lang SA, Goessmann H, Nadalin S, Baumgart J, Farkas SA, et al. Right portal vein ligation combined with in situ splitting induces rapid left lateral liver lobe hypertrophy enabling 2-staged extended right hepatic resection in small-for-size settings. Ann Surg 2012;255:405-414.
8. Garcia-Perez R, Revilla-Nuin B, Martines CM, Bemabe-Garcia A, Mazo, AB, Paricio PP. Associated Liver Partition and Portal Vein Ligation (ALPPS) vs Selective Portal Vein Ligation (PVL) for Staged Hepatectomy in a rat model. Similar regenerative response? PLoS One 2015;10:e0144096.
9. Shi H, Yang G, Zheng T, Wang J, Li L, Liang Y, et al. A preliminary study of ALPPS procedure in a rat model. Sci Rep 2015;5:17567.
10. Kron P, Linecker M, Limani P, Schlegel A, Kambakamba P, Lehn JM, et al. Hypoxia-driven Hif2a coordinates mouse liver regeneration by coupling parenchymal growth to vascular expansion. Hepatology 2016;64:2198-2209.
11. Schadde E, Tsatsaris C, Swiderska-Syn M, Breitenstein S, Urner M, Schimmer R, et al. Hypoxia of the growing liver accelerates regeneration. Surgery 2017;161:666-679.
12. Schlegel A, Lesurtel M, Melloul E, Limani P, Tschuor C, Graf R, et al. ALPPS: from human to mice highlighting accelerated and novel mechanisms of liver regeneration. Ann Surg 2014;260:839-846.
13. Langiewicz M, Schlegel A, Saponara E, Linecker M, Borger P, Graf R, Humar B, Clavien PA. Hedgehog pathway mediates early acceleration of liver regeneration induced by a novel two-staged hepatectomy in mice. J Hepatol 2017;66:560-570.
14. Friedman SL. Evolving challenges in hepatic fibrosis. Nat Rev Gastroenterol Hepatol 2010;7:425-436.
15. Swiderska-Syn M, Xie G, Michelotti GA, Jewell ML, Premont RT, Syn WK et al. Hedgehog regulates Yes-Associated Protein 1 in regeneration mouse liver. Hepatology 2016;64:232-244.
16. Michelotti GA, Xie G, Swiderska M, Choi SS, Karaca G, Kruger L, et al. Smoothened is a master regulator of adult liver repair. J Clin Invest 2013;126:2380-2394.
17. Swiderska-Syn M, Syn WK, Xie G, Kruger L, Machado MV, Karaca G, et al. Myofibroblastic cells function as progenitors to regenerate murine livers after partial hepatectomy. Gut 2014;63:1333-1344.

18. Ochoa B, Syn WK, Delgado I, Karaca GF, Jung Y, Wang J, et al. Hedgehog signaling is critical for normal liver regeneration after partial hepatectomy in mice. Hepatology 2010;51:1712-1723.
19. Lehman K, Tschuor C, Rickenbacher A, Jang JH, Oberkofler CE, Tschopp O, et al. Liver failure after extended hepatectomy in mice is mediated by a p21-dependent barrier to liver regeneration. Gastroenterology 2012; 143:1609-1619.
20. DeLeve LD, Wang X, Guo Y. Sinusoidal endothelial cells prevent rat stellate cell activation and promote reversion to quiescence. Hepatology 2008;48:920-930.
21. Mabuchi A, Mullaney I, Sheard P, Hessian P, Zimmerman A, Senoo H et al. Role of hepatic stellate cells in the early phase of liver regeneration in rat: formation of tight adhesion to parenchymal cells. Comp Hepatol 2004;3:S29.
22. Seki E, Brenner DA, Karin M. A liver full of JNK: signaling in regulation of cell function and disease pathogenesis, and clinical approaches. Gastroenterology 2012;142:307-320.
23. Davies C, Tournier C. Exploring the function of the JNK (c-Jun N-terminal kinase) signaling pathway in physiological and pathological processes to design novel therapeutic strategies. Biochem Soc Trans 2012;40:85-89.
24. Farzan SF, Singh S, Schilling NS, Robbins DJ. The adventures of sonic hedgehog in development and repair. III Hedgehog processing and biological activity. Am J Physiol Gastrointest Liver Physiol 2008;294:G844-G849.
25. Ingham PW, McMahon AP. Hedgehog signaling in animal development: paradigms and principles. Genes & Dev 2001;15:3059-3087.
26. Kluwe J, Pradere JP, Gwak GY, Mencin A, Minicis SD, Osterreicher CH et al. Modulation of hepatic fibrosis by c-Jun-N-terminal kinase inhibition. Gastroenterology 2010;138:347-359.
27. Bennet BL, Sasaki DT, Murray BW, O'Leary EC, Sakata ST, Xu W et al. SP600125, an anthrapyrazolone inhibitor of Jun N-terminal kinase. Proc Natl Acad Sci USA 2001;98:13681-13686.
28. Schwabe RF, Bradham CA, Uehara T, Hatano E, Bennet BL, Schoonhoven R, et al. c-Jun-N-terminal kinase drives cyclin D1 expression and proliferation during liver regeneration. Hepatology 2003;37:824–832.
29. Michalopoulos GK. Liver regeneration. J Cell Physiol 2007;213:286-300.
30. Westwick JK, Weitzel C, Leffert HL, Brenner DA. Activation of Jun kinase is an early event in hepatic regeneration. J Clin Invest 1995;95:803-810.
31. Alcorn JA, Feitelberg SP, Brenner DA. Transient induction of c-jun during hepatic regeneration. Hepatology 1990;11:909–915.
32. Schnabl B, Bradham CA, Bennett BL, Manning AM, Stefanovic B, Brenner DA. TAK1/JNK and p38 have opposite effects on rat hepatic stellate cells. Hepatology 2001;34:953–963.
33. Omenetti A, Choi S, Michelotti G, Diehl AM. Hedgehog signaling in the liver. J Hepatol 2011;54:366-373.
34. Laner-Plamberger S, Kaser A, Paulischta M, Hauser-Kronberger C, Eichberger T, Frischauf AM. Cooperation between GLI and JUN enhances transcription of JUN and selected GLI target genes. Oncogene 2009;2:1639-1651.
35. Schwabe RF, Brenner DA. Mechanisms of Liver Injury. I. TNF-alpha-induced liver injury: role of IKK, JNK, and ROS pathways. Am J Physiol Gastrointest Liver Physiol 2006;290:G583-589.
36. Gunawan BK, Liu ZX, Han D, Hanawa N, Gaarde WA, Kaplowitz N. c-Jun N-terminal kinase plays a major role in murine acetaminophen hepatotoxicity. Gastro 2006;131:165-178.
37. Choi SS, Omenetti A, Syn WK, Diehl AM. The role of hedgehog signaling in fibrogenic liver repair. Int J Biochem Cell Biol 2011;43:238-44.

38. Luo JD, Hu TP, Wang L, Chen MS, Liu SM, Chen AF. Sonic hedgehog improves would healing via enhancing cutaneous nitric oxide function in diabetes. Am J Physiol Endocrinol Metab 2009;297:E525-531.
39. Boege Y, Malehmir M, Healy ME, Betterman K, Lorentzen A, Vucur M et al. A dual role of caspase-8 in triggering and sensing proliferation-associated DNA damage, a key determinant of liver cancer development. Cancer Cell 2017;32:342-359.
40. Iansante V, Choy PM, Fung SW, Liu Y, Chai JG, Dyson J, et al. PARP14 promotes the Warburg effect in hepatocellular carcinoma by inhibiting JNK1-dependent PKM2 phosphorylation and activation. Nat Commun 2015;10:7882.
41. Della Corte CM, Viscardi G, Papaccio F, Esposito G, Martini G, Ciardiello D, et al. Implicaiton of the hedgehog pathway in hepatocellular carcinoma. World J Gastroenterol 2017;23:4330-4340.
42. Guy CD, Suzuki A, Zdanowicz M, Abdelmalek MF, Burchette J, Unalp A, et al. Hedgehog pathway activation parallels histologic severity of injury and fibrosis in human nonalcoholic fatty liver disease. Hepatology 2012;55:1711-1721.
43. Behrens A, Sibilia M, David JP, Mohle-Steinlein U, Tronche F, Schutz G et al. Impaired postnatal hepatocyte proliferation and liver regeneration in mice lacking c-jun in the liver. EMBO . 2002;21:1782-1790.
44. Baumgart J, Lang S, Lang H. A new method for induction of liver hypertrophy prior to right trisectionectomy: a report of three cases. HPB (Oxford) 2011;13(Suppl 2):71–72.
45. de Santibanes E, Alvarez FA, Ardiles V. How to avoid postoperative liver failure: a novel method. World J Surg 2012;36:125–128.
46. Alvarez FA, Iniesta J, Lastiri J, Ulla M, Bonadeo Lassalle F, de Santibanes E. New method of hepatic regeneration. Cir Esp 2011;89:645–649.

Figure Legends

Figure 1. JNK1 is upregulated early after ALPPS. *(A)* In-silico analysis linking components of the hedgehog pathways to *Mapk8* (JNK1) by the String database. Green lines represent suspected links between genes from their database of publications. Blue and pink lines represent experimentally determined links between genes. *(B)* Raw hepatic gene expression values of *Mapk8* from RNA sequencing data and corresponding qPCR validation. *(C)* Hepatic protein expression (normalized to GAPDH) of JNK1 and pJNK1 after surgery. N=5/group, t-test, *P<0.05, ** P<0.01. ***P<0.001. Significances refer to ALPPS vs. PVL comparison.

Figure 2. JNK1/IHH cellular location and associated downstream signaling in liver *(A)* pJNK1/alpha-SMA and pJNK1/Ihh immunofluorescence co-stain showing co-localization of both proteins in nonparenchymal cells (see Supplementary Figure 1 and 2 for stainings in control surgeries) . *(B)* Cytosolic and nuclear protein levels (normalized to β-tubulin and lamin B1, respectively; see immunoblots in Supplementary Figure 16) of pJNK1, GLI1, and Cyclin D. *(C)* Counts of cyclin D, Ki67, and bold pH3-positive hepatocyte nuclei hepatocyte counts(see Supplementary Figure 4 for corresponding stains). . N=5/group. t-test, *P<0.05,** P<0.01, ***P<0.001. Significances refer to ALPPS vs. PVL comparison.

Figure 3. JNK1 inhibition reduces the regenerative speed after ALPPS. *(A)* Cytosolic and nuclear pJNK1 levels (normalized to β-tubulin and lamin B1, respectively; see Supplementary Fig. 16 for immunoblots in). N=5/group. *(B)* Body weight and liver weight regain (expressed as percent FLR/BW) after surgery and treatment with SP600125 are shown in the left and right graph, respectively. *(C)* Corresponding Ki67 and pH3 counts (see Supplementary Fig. 6 for stains). N=5/group, t-test, *P<0.05, **P<0.01, ***P<0.001 for ALPPS + DMSO *versus* ALPPS + SP6 unless otherwise indicated.

Figure 4. JNK1 inhibition dpwnregulates the IHH pathway after ALPPS. *(A)* Plasma IHH levels (ELISA) and hepatic protein expression (normalized to GAPDH) after surgery and treatment. Hepatic gene expression of *(B) Gli1* and *(C) Hhip* after surgery and treatment. *(D)* Cytosolic and nuclear protein

levels (normalized to β-tubulin and lamin B1, respectively) of GLI1 and Cyclin D. *(E)* Immunofluorescence for hepatic GLI1. Note that SP600125 treatment reduces nuclear staining in hepatocytes. (*F*) Cyclin D counts (see Supplementary Fig. 9 for stains). N=5/group, t-test, *P<0.05, **P<0.01, ***P<0.001 for ALPPS + DMSO vs ALPPS + SP6.

Figure 5. Effects of JNK1 inhibition combined with recombinant IHH treatment on regeneration after ALPPS. *(A)* Body weight and liver weight (FLR/BW) after ALPPS+ SP6 with/without rIHH *versus* corresponding vehicle controls and ALPPS or PVL alone. *(B)* Corresponding Ki67 and pH3 counts (see Supplementary Fig. 10 for stain). N=5/group, t-test, *P<0.05, **P<0.01, ***P<0.001 for ALPPS + SP6 *versus* ALPPS + SP6 and recombinant Ihh.

Figure 6. Effects of JNK1 inhibition combined with recombinant IHH treatment on hedgehog signaling after ALPPS. *(A)* Hepatic gene expression of *Gli1* and *Hhip* after surgery and treatment. *(B)* Cytosolic and nuclear protein levels (normalized to β-tubulin and lamin B1, respectively) of GLI1 and Cyclin D. *(C)* Immunofluorescence for hepatic GLI1. Note the restoration of nuclear GLI1 expression in SP600125-treated liver through rIHH. *(D)* Cyclin D nuclear counts see Supplementary Figure 11 for stains) *(E)* Cytosolic and nuclear protein levels of pJNK1. N=5/group, t-test, *P<0.05, **P<0.01, ***P<0.001 for ALPPS + SP6 *versus* ALPPS + SP6 and rIHH.

Supplementary Information

JNK1 induces IHH signaling from stellate cells to accelerate liver regeneration after ligation and transection in mice

Magda Langiewicz[1], Rolf Graf[1], Bostjan Humar[1*], and Pierre A. Clavien[1*].

*shared senior authorship

Affiliations: [1]Department of Surgery, Swiss Hepato-Pancreato-Biliary (HPB) and Transplantation Center, University Hospital Zurich, Raemistrasse 100, Zurich, CH-8091, Switzerland.

Supplementary Information

- Supplementary Materials & Methods
- Supplementary Tables
- Supplementary Figures
- Supplementary References
- Supplementary File Western Blots

Supplementary Materials & Methods

Quantitative real-time PCR

Total RNA was extracted from 50 mg of tissue using Trizol reagent following provided instructions (Invitrogen, Basel, Switzerland). RNA quality/quantity was spectrometrically assessed. qPCR was performed with two replicates/sample on cDNA (Thermo Script reverse transcription PCR System, Invitrogen) using an ABI Prism 7500 Sequence Detector system (PE Applied Biosystems Rotkreuz, Switzerland). Taqman gene expression assays from Applied Biosystems are listed in Supplementary Table 1. Results represent mean fold induction ($2^{-\Delta Ct}$) ±SD relative to the normalization control *18S rRNA*.[1]

Histological Examination

Archived liver sections (3 µm) were stained (antibodies in Supplementary Table 2) using the Dako Autostainer Link48 Instrument and the iView DAB kit (Dako Denmark A/S). Quantification of Ki67-, bold pH3-, [1] cyclin D-, and pJNK-positive hepatocytes was achieved by blinded manual counting in 10 random visual fields (20x). For immunofluorescence, GLI1 antibody (R&D, Zug, Switzerland) was detected using an Alexa Fluor 488-conjugated anti-rat secondary antibody (Invitrogen, Zug, Switzerland). For co-immunofluorescence, primary antibodies are listed in Supplementary Table 2 and rabbit- and mouse-specific Alexa Fluor 488 and 594-conjugated secondary antibodies were used respectively. Representative slides of five biological samples per group are shown.

Supplementary Tables

Table S1. Taqman gene expression assays

gene name	Applied Biosystems order no.
Gli1	Mm00494654_m1
Gli2	Mm01293117_m1
Hhip	Mm00469580_m1
Mapk8	Mm00489514_m1
Mapk9	Mm_00444231_m1
Mapk10	Mm_00436518_m1
Ptch1	Mm00436026_m1
Smo	Mm01162710_m1
18S rRNA	Control reagents

Table S2. Antibodies

Antigene	Company (order no.)	Dilution
Ki67	Abcam, Cambridge, UK (ab16667)	1:200 (IHC)
pH3	Millipore, Schaffhausen, CH (06-570)	1:500 (IHC)
Gli1	R&D, Zug, CH (Mab3324)	1:50 (IF) 1:5000 (WB)
Gli2	Abcam, Cambridge, UK (ab26056)	1:500 (WB)
cyclin D	Abcam, Cambridge, UK (ab16663)	1:100 (IHC) 1:100 (WB)
Alpha-SMA	Abcam, Cambridge, UK (ab32575)	(IF)
pJNK	Santa Cruz, CA USA (sc6254)	1:50 (IF)
pJNK	R&D, Zug, CH (AF1205)	(IHC)
Ihh	Abcam, Cambridge, UK (ab39634)	1:250 (IF) 1:500 (IHC)
lamin B1	Santa Cruz, CA USA (sc-377001)	1:500 (WB)
β-tubulin	Cell Signaling, MA USA (2128S)	1:1000 (WB)

Supplementary Figures

Figure S1. Serum injury levels and Mapk9/10 expression after ALPPS and control surgeries.

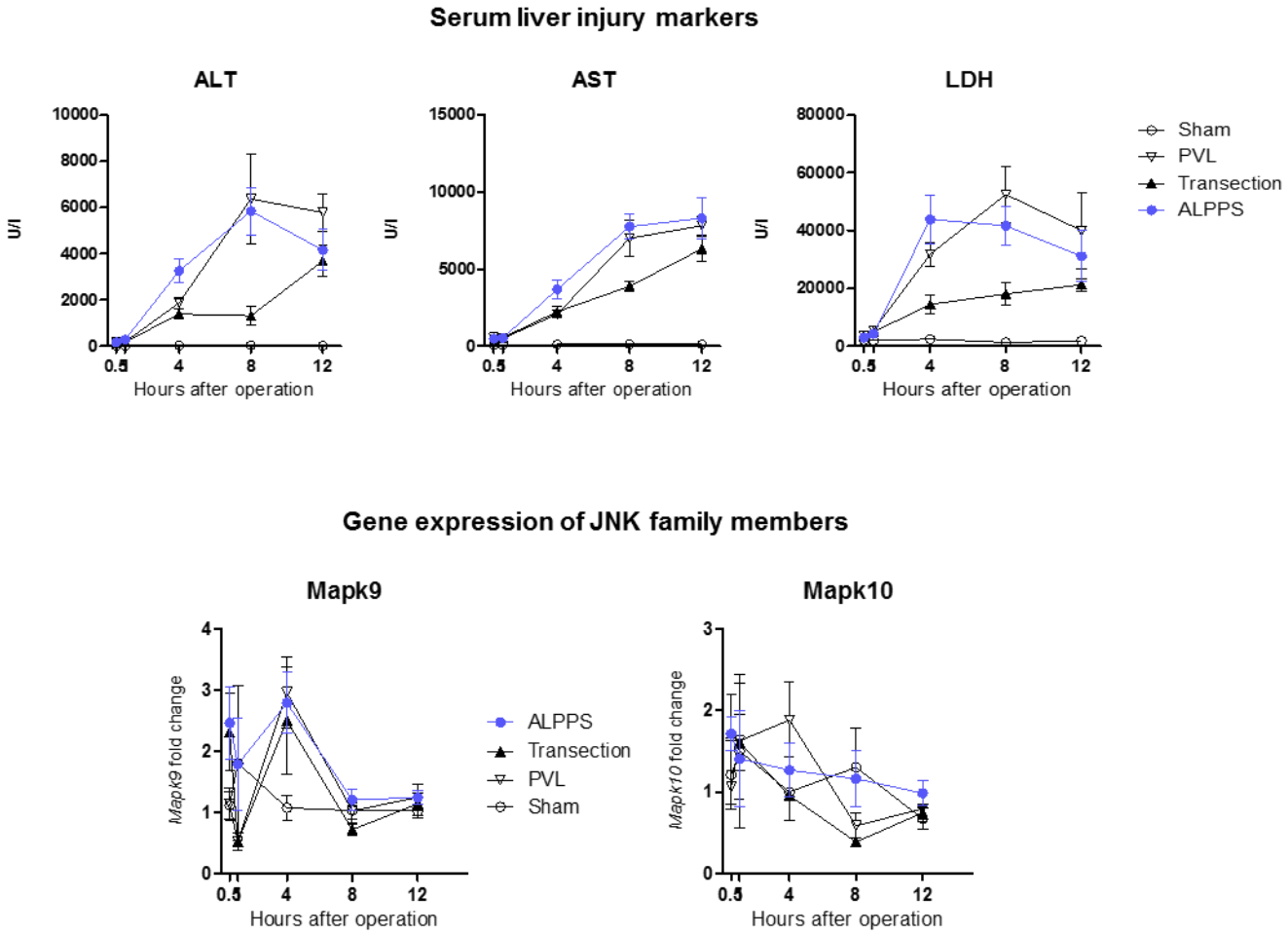

Supplementary Figure 1. Upper graphs: serum ALT, AST and LDH levels after surgeries suggest similar injury levels after ALPPS and PVL surgery. Lower graphs: Gene expression for the JNK family members JNK2 and JNK3 (*Mapk9*, *Mapk10*) as assessed by qPCR.

Figure S2. Immunohistochemistry for IHH, ASMA, and pJNK1 on liver post surgery.

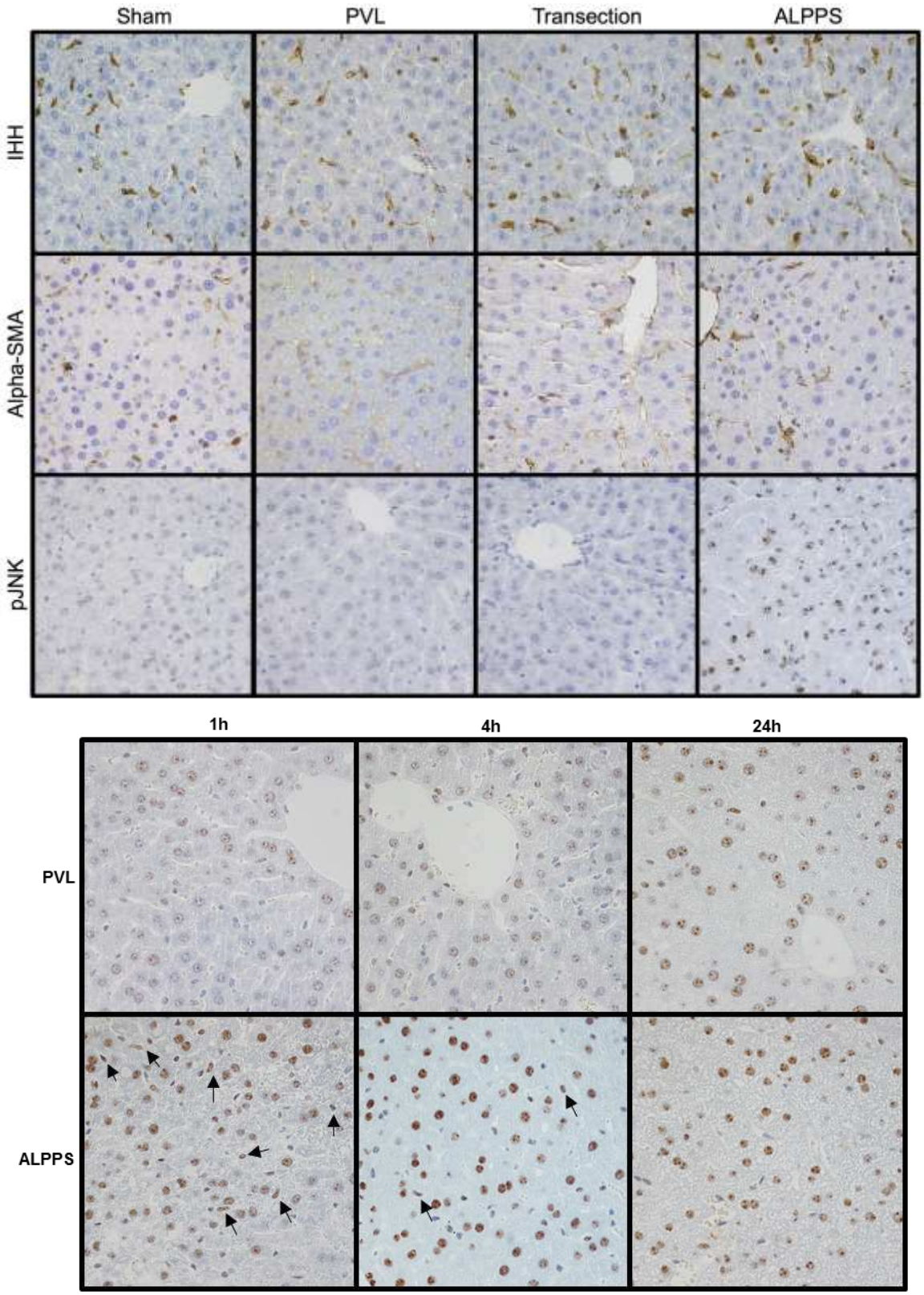

Supplementary Figure 2. Representative immunostainings for IHH, ASMA, and pJNK1 on liver at four hours after ALPPS, PVL, transection, and sham operations. Below images show pJNK1 at different times following PVL or ALPPS surgery. Arrows point to non-parenchymal cells with pJNK1 expression. Note that the immunohistochemical assessment of pJNK1 has to be interpreted with caution, as it did not reflect cytoplasmic expression detected by immunoblots. 40x magnification.

Figure S3. Immunofluorescent co-stains for pJNK1/ASMA and pJNK1/IHH on liver post control surgeries.

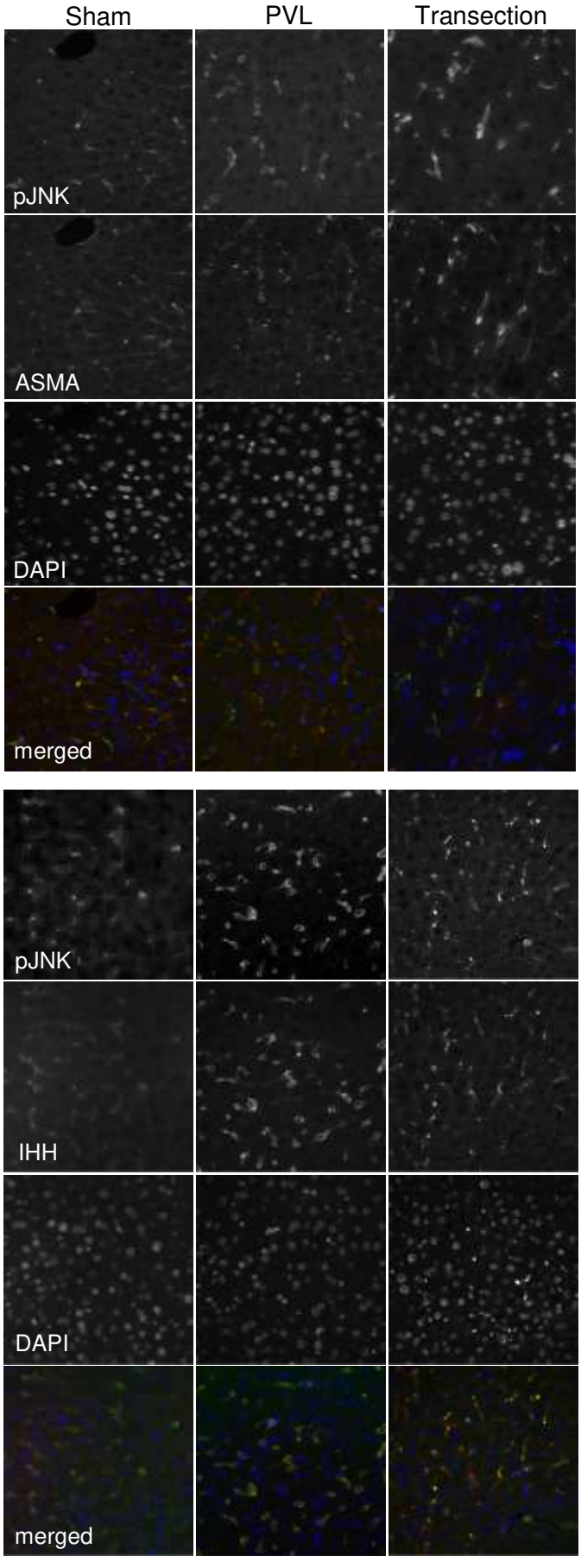

Supplementary Figure 3. Representative immunofluorescent co-stains for pJNK1 and ASMA, and pJNK and IHH on liver four hours after PVL, transection, and sham operations. 40x magnification.

Figure S4. Immunofluorescent co-stains for pJNK1 and IHH on liver post PVL and ALPPS.

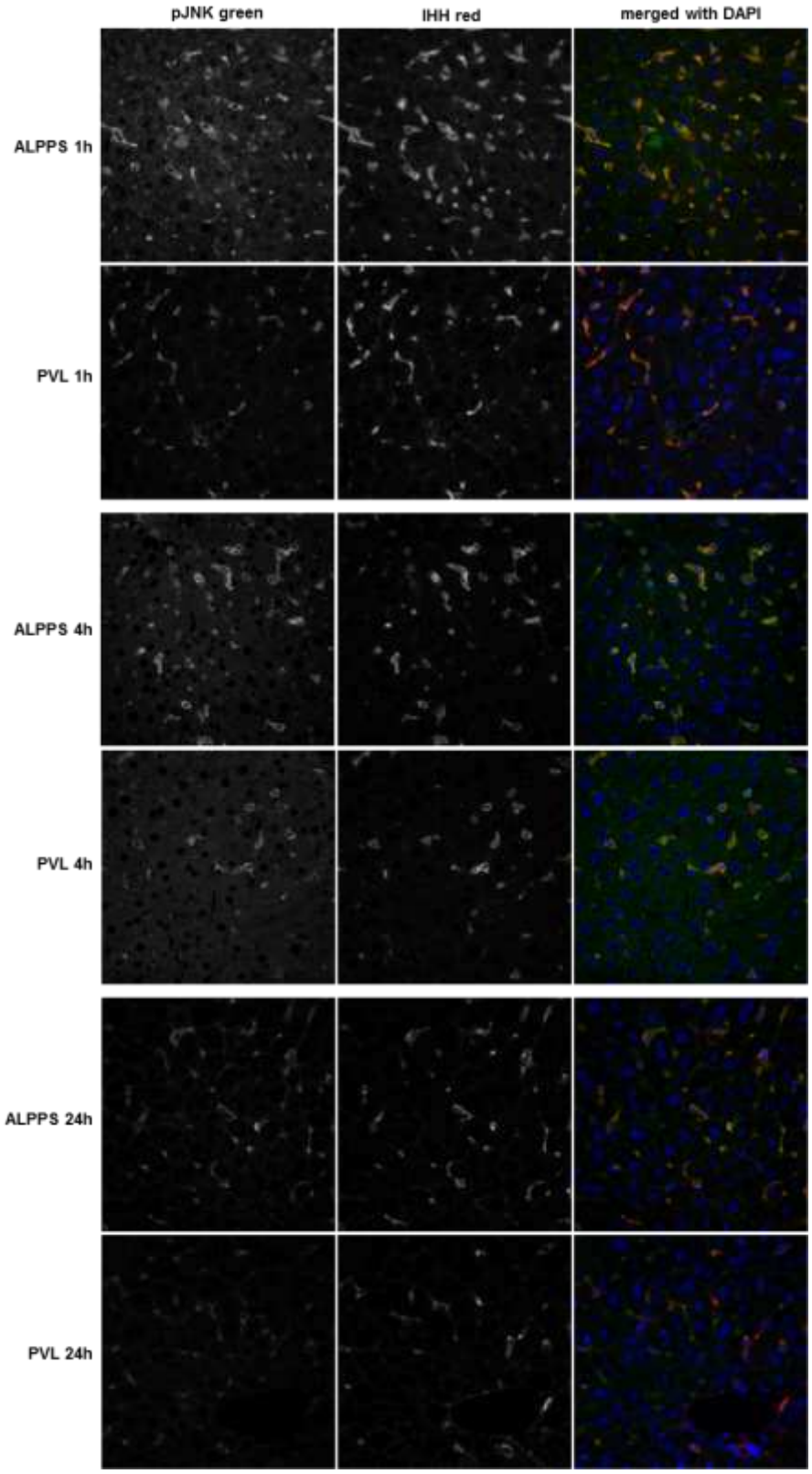

Supplementary Figure 4. Representative immunofluorescent co-stains for pJNK/IHH on liver at 1, 4, and 24 hours after ALPPS or PVL surgery. 40x magnification.

Figure S5. JNK1 and GLI2 protein expression in ALPPS versus control surgeries.

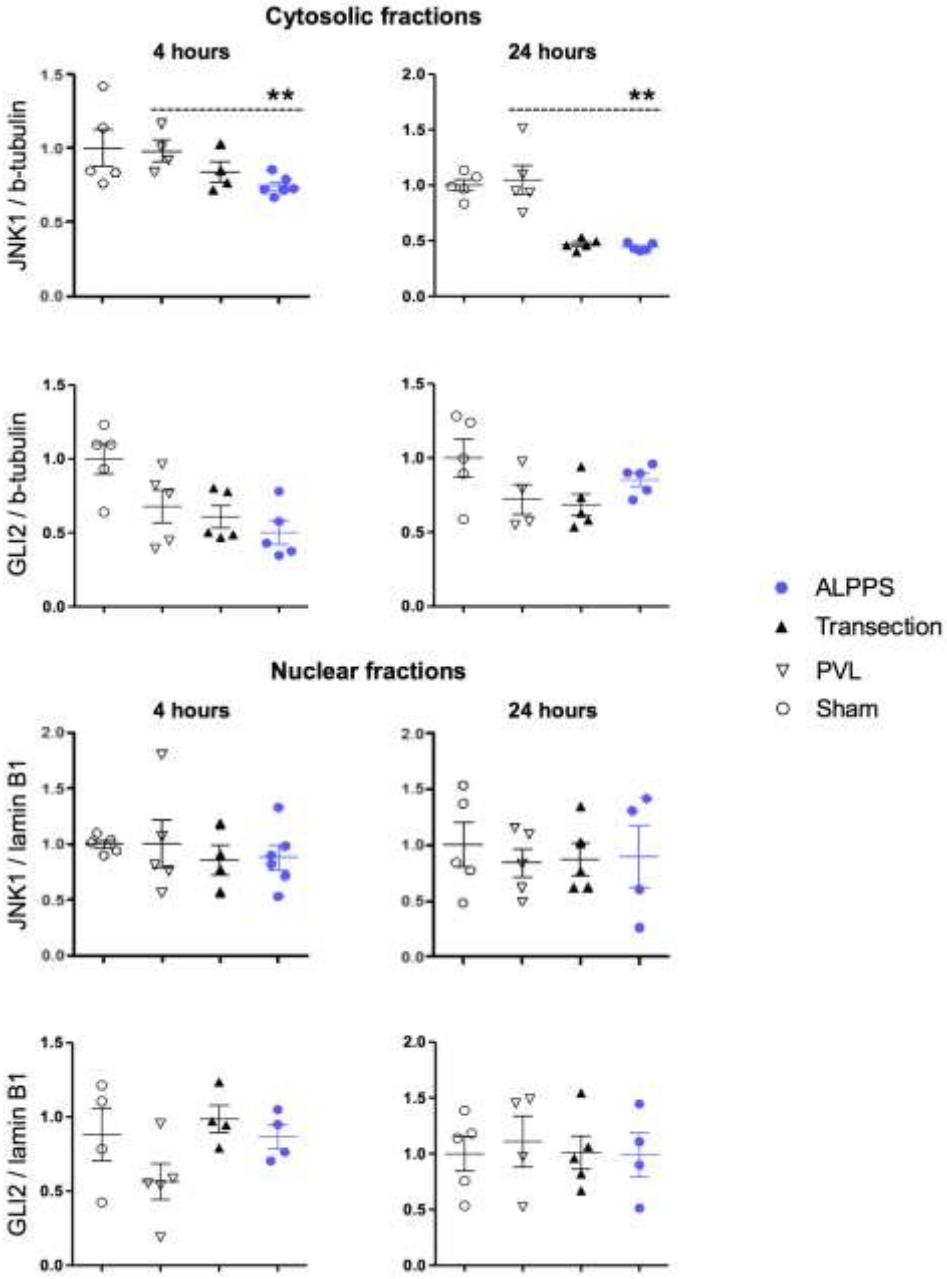

Supplementary Figure 5. JNK1 and GLI2 cytosolic and nuclear protein levels after ALPPS or its surgical controls. N=5 per group. t-test, *P<0.05, **P<0.01. ***P<0.001. Significances refer to ALPPS vs. PVL comparison unless otherwise stated.

Figure S6. H&E staining and immunohistochemistry for Ki67, pH3, and cyclin D on liver post surgery.

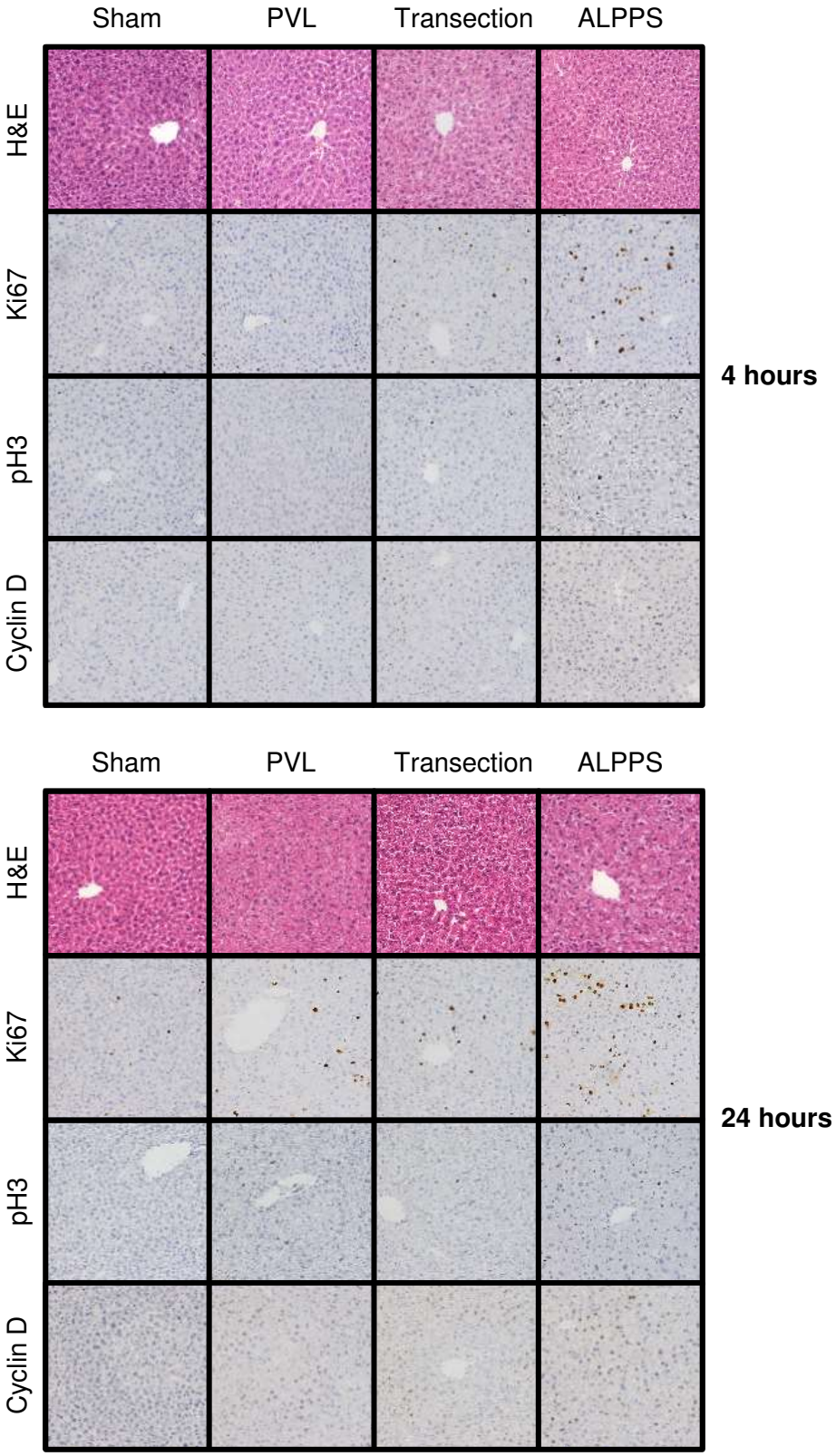

Supplementary Figure 6. Representative immunostainings for H&E, Ki67, pH3, and cyclin 1 on liver after ALPPS, PVL, transection, and sham operations. For pH3, only cells with bold nuclear staining were counted, as these represent mitotic cells.[19] Quantitations are shown in Figure 1E. 20x magnification.

Figure S7. JNK1 nuclear and cytosolic protein levels after JNK inhibition with SP600125.

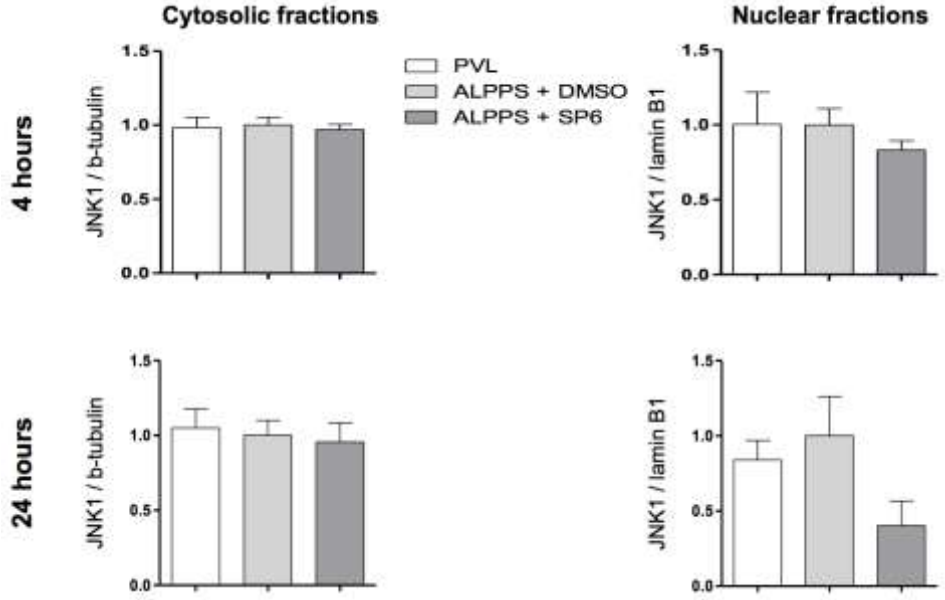

Supplementary Figure 7. JNK1 nuclear and cytosolic protein levels determined by western blot in ALPPS livers with control injection (DMSO) or SP600125. N=5 per group. No significant differences between ALPPS+DMSO and ALPPS+SP6 group comparisons.

Figure S8. Immunohistochemistry for H&E, Ki67, and pH3 on liver after JNK1 inhibition by SP6.

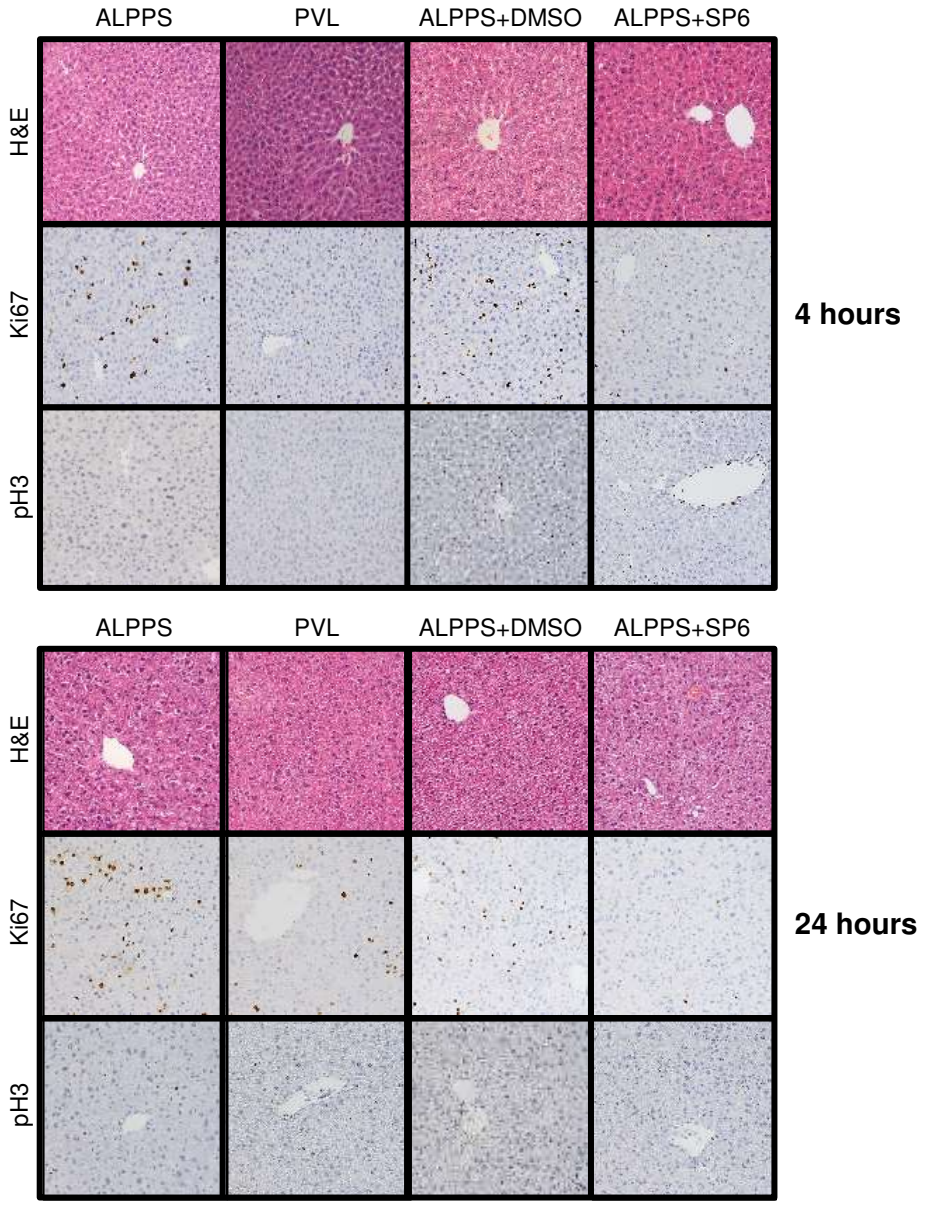

Supplementary Figure 8. Representative immunostainings for H&E, KI67, and pH3 on liver after treatment of ALPPS mice with DMSO, vehicle, or SP600125. 20x magnification.

Figure S9. mRNA analysis of *Smo*, *Ptch1*, *Gli2*, and *Hhip* in livers with JNK1 inhibition by SP6.

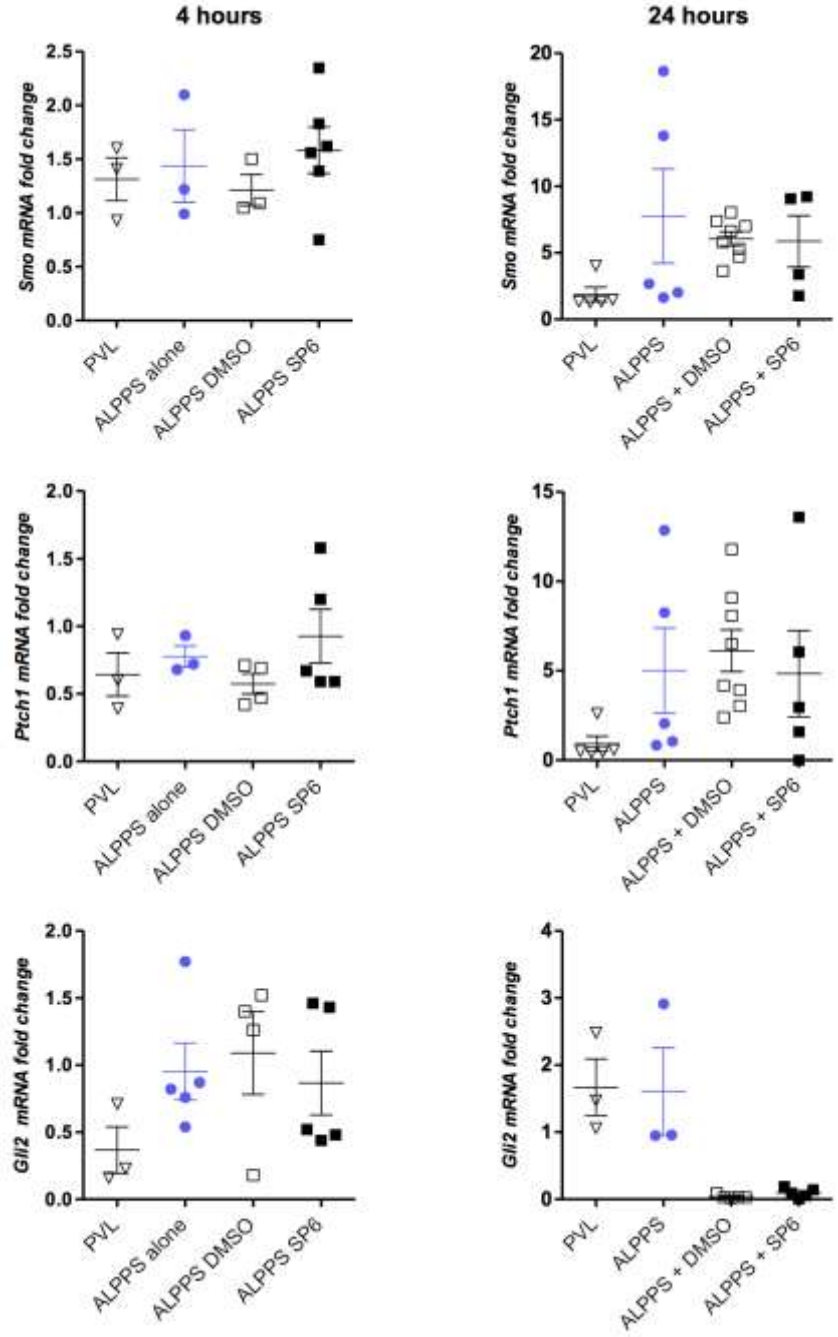

Supplementary Figure 9. mRNA expression analysis of downstream components of IHH signaling in livers with JNK1 inhibition. N=5 per group. No significant differences between ALPPS+DMSO and ALPPS+SP6 group comparison.

Figure S10. GLI2 protein levels in livers with JNK1 inhibition by SP6.

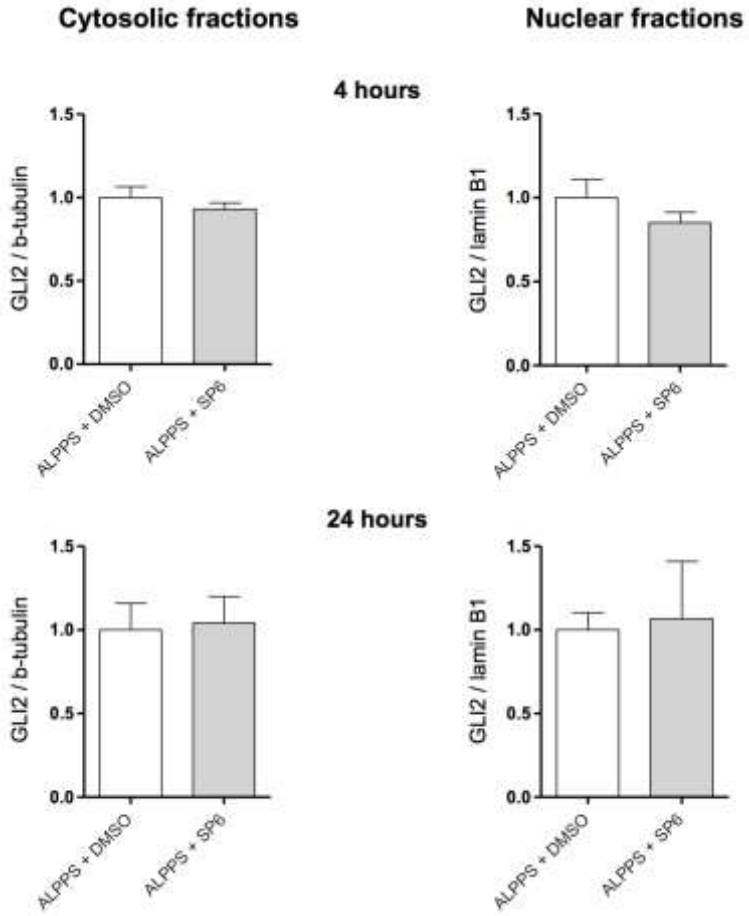

Supplementary Figure 10. Hepatic GLI2 protein levels in nuclear and cytosolic fractions after vehicle (DMSO) or SP600125 treatment followed by ALPPS. N=5 per group. No significant differences between ALPPS+DMSO and ALPPS+SP6 group comparison.

Figure S11. Immunohistochemistry for cyclin D1 on liver after JNK1 inhibition by SP6.

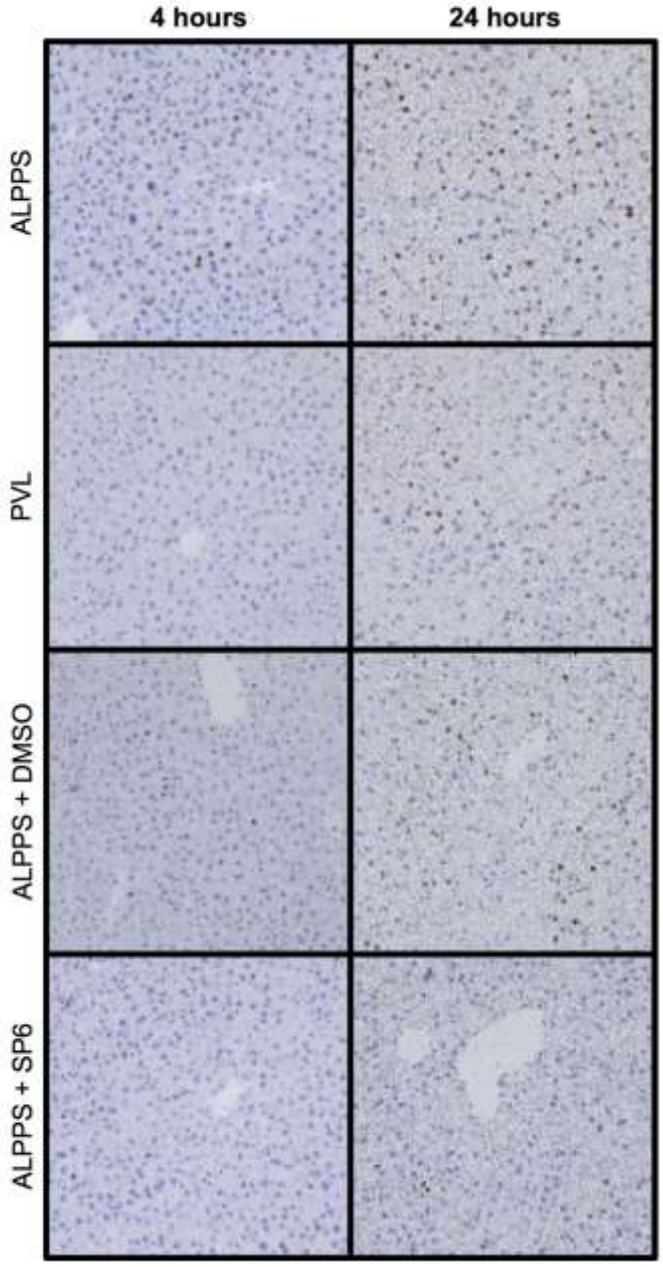

Supplementary Figure 11. Representative immunostainings for pJNK and cyclin D on liver after treatment of ALPPS mice with DMSO vehicle or SP600125. 20x magnification.

Figure S12. Immunohistochemistry for H&E, Ki67, and pH3 on livers with JNK1 inhibition by SP6 and recombinant IHH treatment.

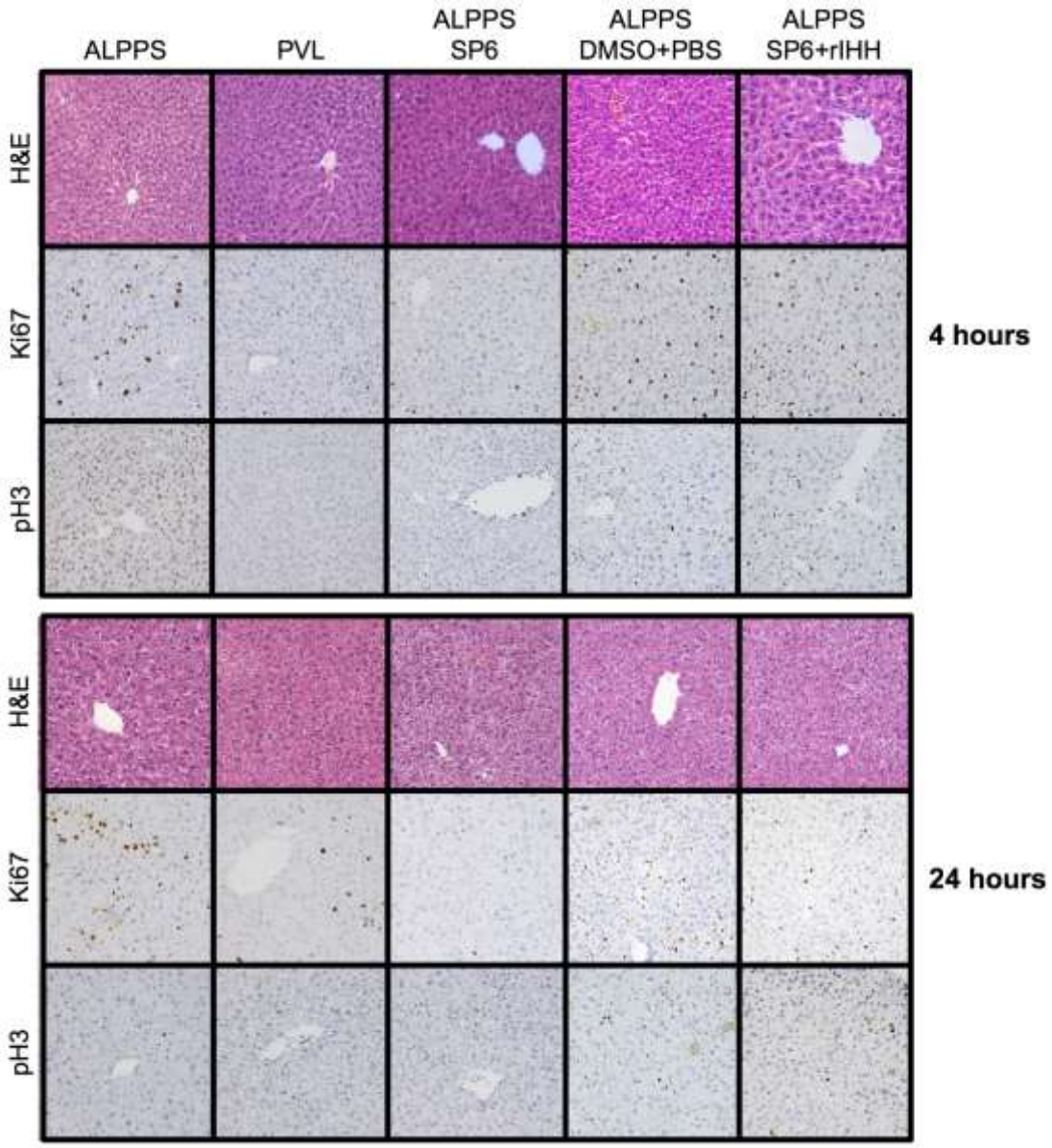

Supplementary Figure 12. Representative immunostainings for H&E, KI67, and pH3 on liver after treatment of ALPPS mice with vehicle injections (DMSO and PBS), or SP600125, or SP600124 and recombinant IHH injections. 20x magnification.

Figure S13. Immunohistochemistry for cyclin D on liver after JNK1 inhibition and recombinant IHH treatment.

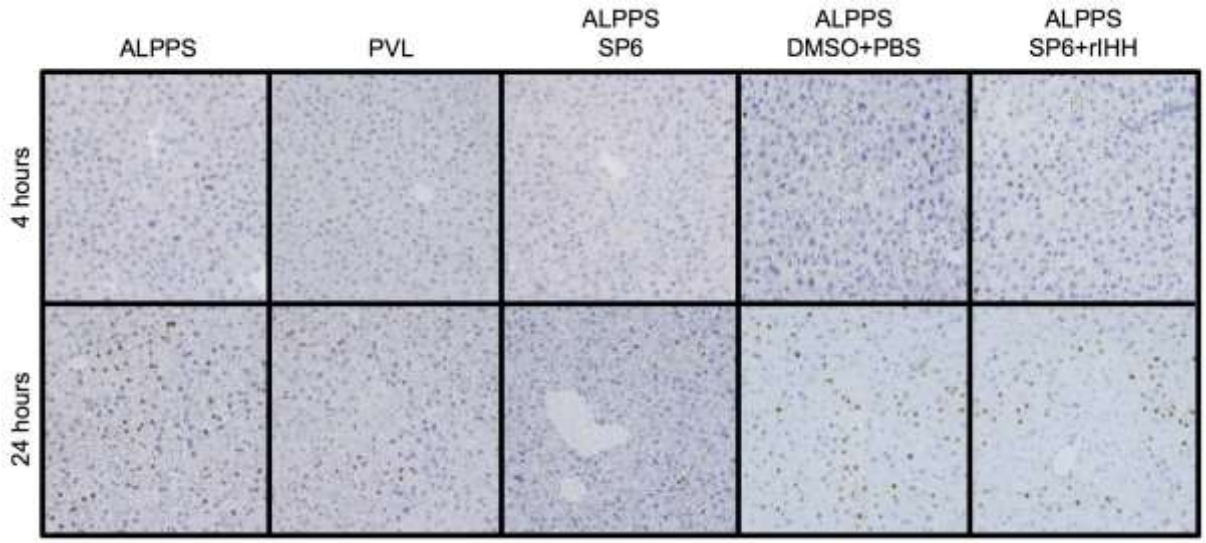

Supplementary Figure 13. Representative immunostainings for pJNK and cyclin D1 on liver after treatment of ALPPS mice with vehicle (DMSO and PBS), or SP600125, or SP600125 and recombinant IHH treatment. 20x magnification.

Figure S14. mRNA analysis of *Ptch1*, *Smo*, *Gli2*, and *Hhip* in livers with JNK1 inhibition and recombinant IHH treatment.

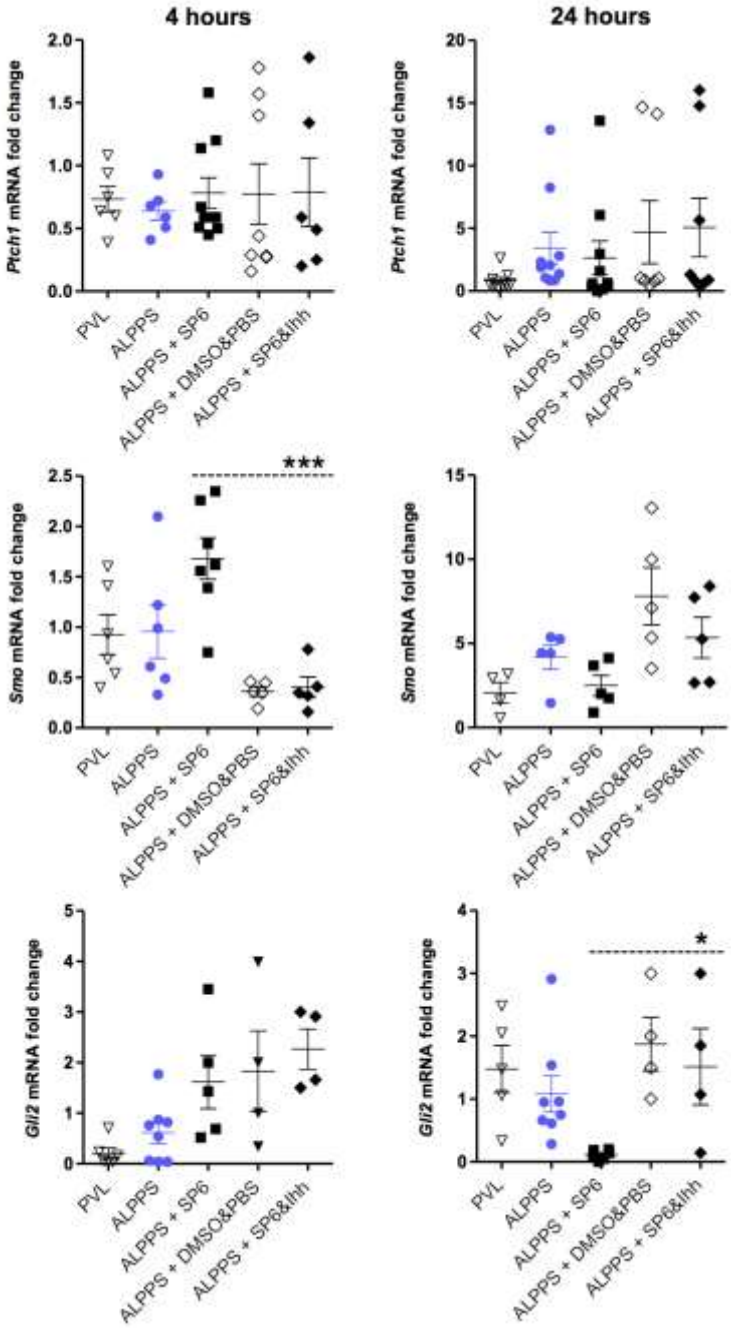

Supplementary Figure 14. mRNA expression analysis of downstream components of IHH signaling in livers with JNK inhibition and recombinant IHH treatment. N=5 per group. t-test, *P < 0.05, **P < 0.01. ***P < 0.001. Significances refer to ALPPS+SP6 vs. ALPPS+SP6+rIHH comparison. Note that the significant changes in *Smo* expression were not further analyzed, as *Smo* gene expression correlated neither with regenerative responses nor with GLI1 activation.

Figure S15. GLI2 protein levels in livers with JNK1 inhibition and recombinant IHH treatment.

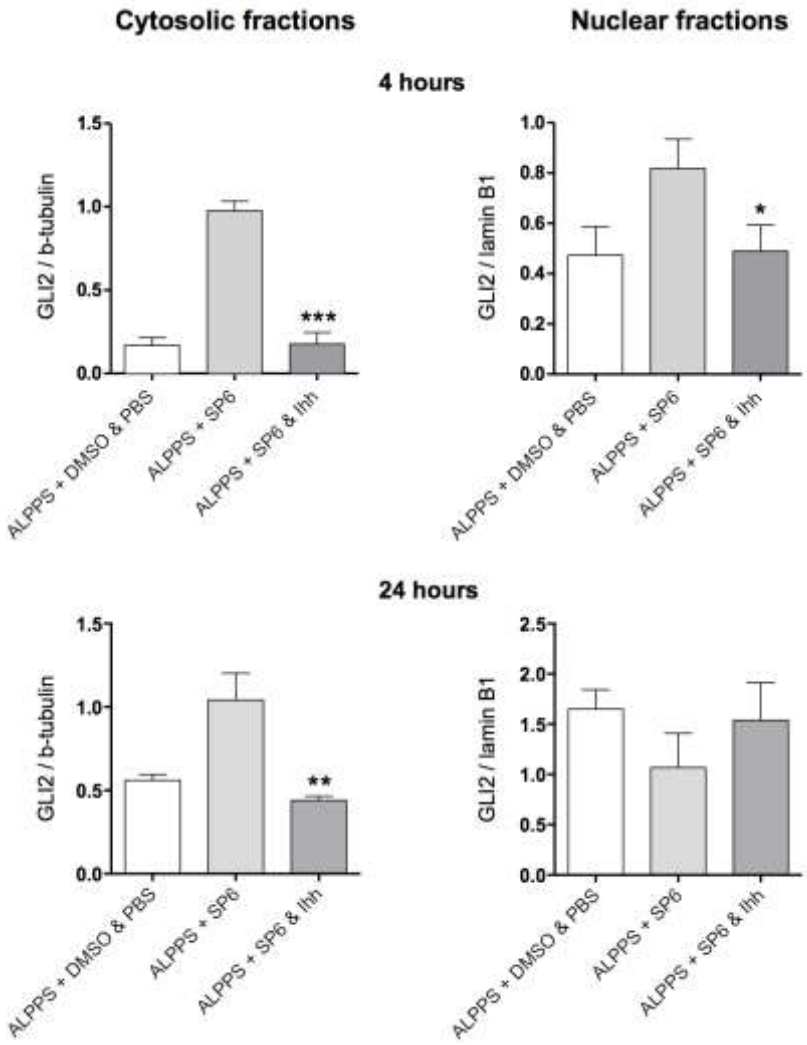

Supplementary Figure 15. GLI2 protein levels in nuclear and cytosolic fractions in livers with vehicle (DMSO&PBS), or SP600125, or SP600125 and recombinant IHH treatment. The significant downregulation of nuclear GLI2 through IHH treatment further corroborates that GLI2 does not contribute to the JNK1-IHH axis in ALPPS. N=5 per group. t-test, *P < 0.05, **P < 0.01. ***P < 0.001. Significances refer to ALPPS+SP6 vs. ALPPS+SP6+rIHH comparison.

Figure S16. JNK1 protein levels in livers after JNK loss treatment and recombinant Ihh treatment.

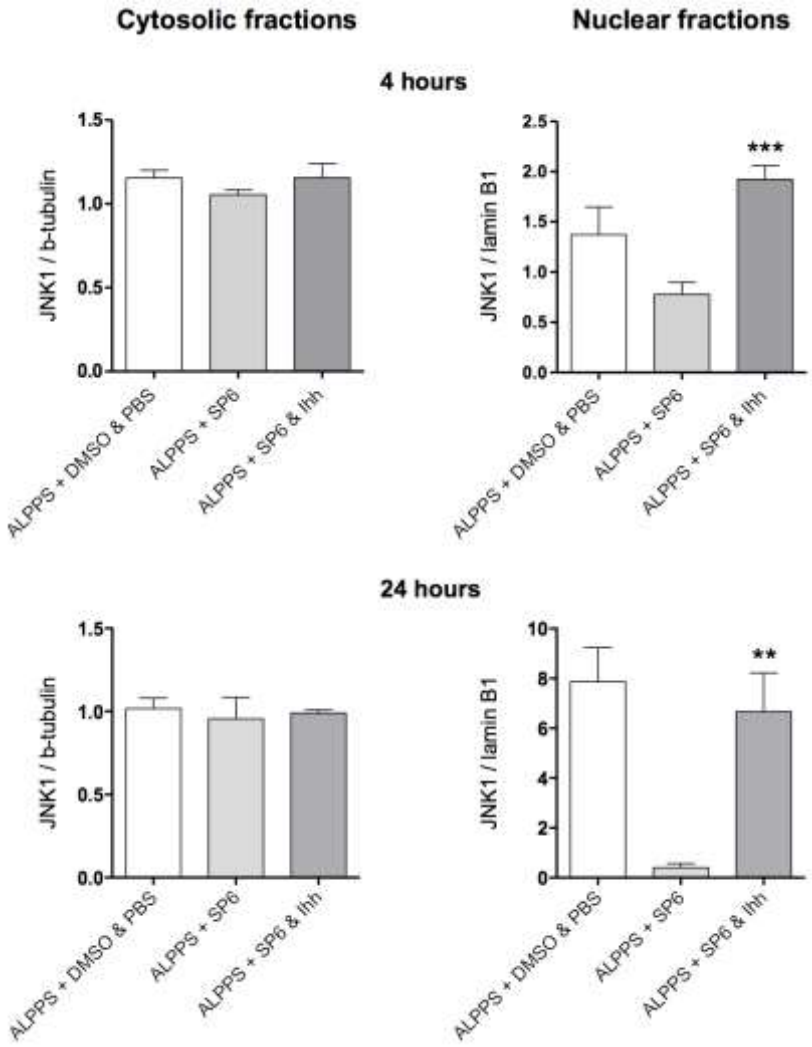

Supplementary Figure 16. JNK1 protein levels in nuclear and cytosolic fractions in livers of ALPPS mice treated with vehicle injection (DMSO & PBS), or SP600125, or SP600125 and recombinant IHH (referring to Figure 6E). N=5 per group. t-test, *P < 0.05, **P < 0.01. ***P < 0.001. Significances refer to ALPPS+SP6 vs. ALPPS+SP6+rIHH comparison.

Figure S17. Immunohistochemistry for pJNK1 on liver after JNK1 inhibition and recombinant IHH treatment.

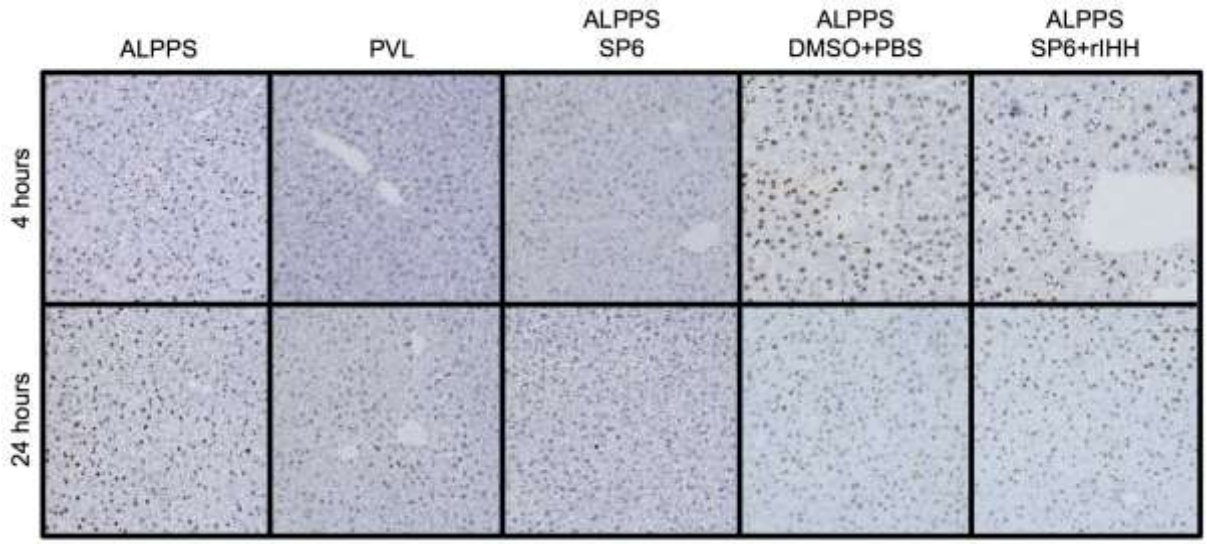

Supplementary Figure 17. Representative immunostainings for pJNK1 on liver after treatment of ALPPS mice with vehicle (DMSO and PBS), or SP600125, or SP600125 and recombinant IHH treatment. 20x magnification.

Figure S18. Immunofluorescence for pJNK1 and IHH on liver after PVL and PBS injection or rIHH injection.

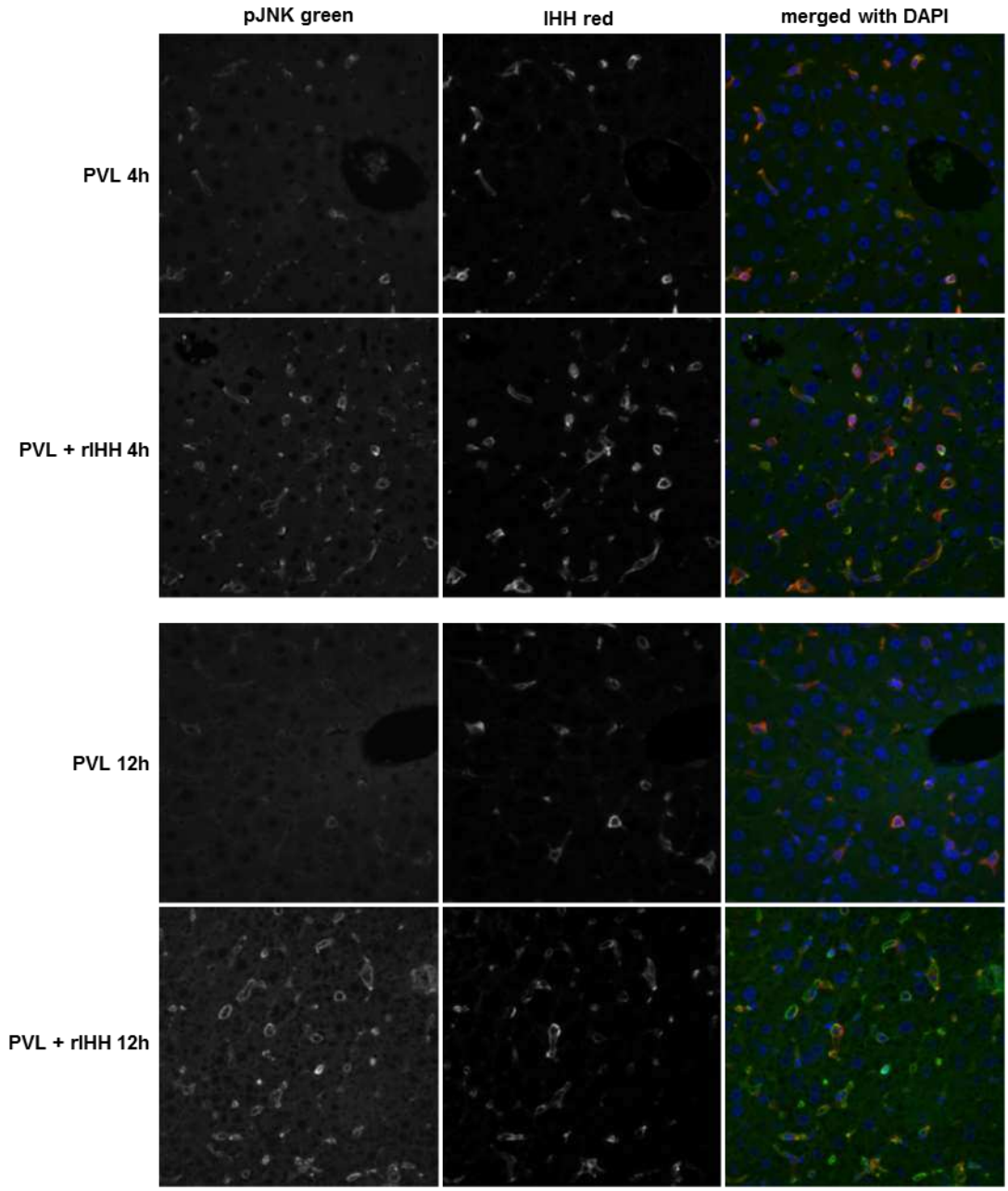

Supplementary Figure 18. Representative immunostainings for pJNK1 and IHH at 4h and 12h after PVL surgery with concomitant injection of PBS (control) or rIHH. We have previously shown that rIHH treatment of PVL mice induces GLI1-cyclin D1, promotes hepatocellular proliferation, and accelerates regeneration to levels observed in ALPPS mice, demonstrating the central role of IHH in ALPPS.[2] Relative to controls, rIHH also elevated pJNK expression in stellate cells, provding further evidence for a positive feedback loop between IHH and JNK1.

Supplementary References

1. Lehman K, Tschuor C, Rickenbacher A, Jang JH, Oberkofler CE, Tschopp O, et al. Liver failure after extended hepatectomy in mice is mediated by a p21-dependent barrier to liver regeneration. Gastroenterology 2012; 143:1609-1619.
2. Langiewicz M, Schlegel A, Saponara E, Linecker M, Borger P, Graf R, Humar B, Clavien PA. Hedgehog pathway mediates early acceleration of liver regeneration induced by a novel two-staged hepatectomy in mice. J Hepatol 2017;66:560-570.

Supplementary File Immunoblots. Western blot images for all protein expression experiments for JNK, pJNK, IHH, GLI1, GLI2, and cyclin D for all treatment and surgical groups.

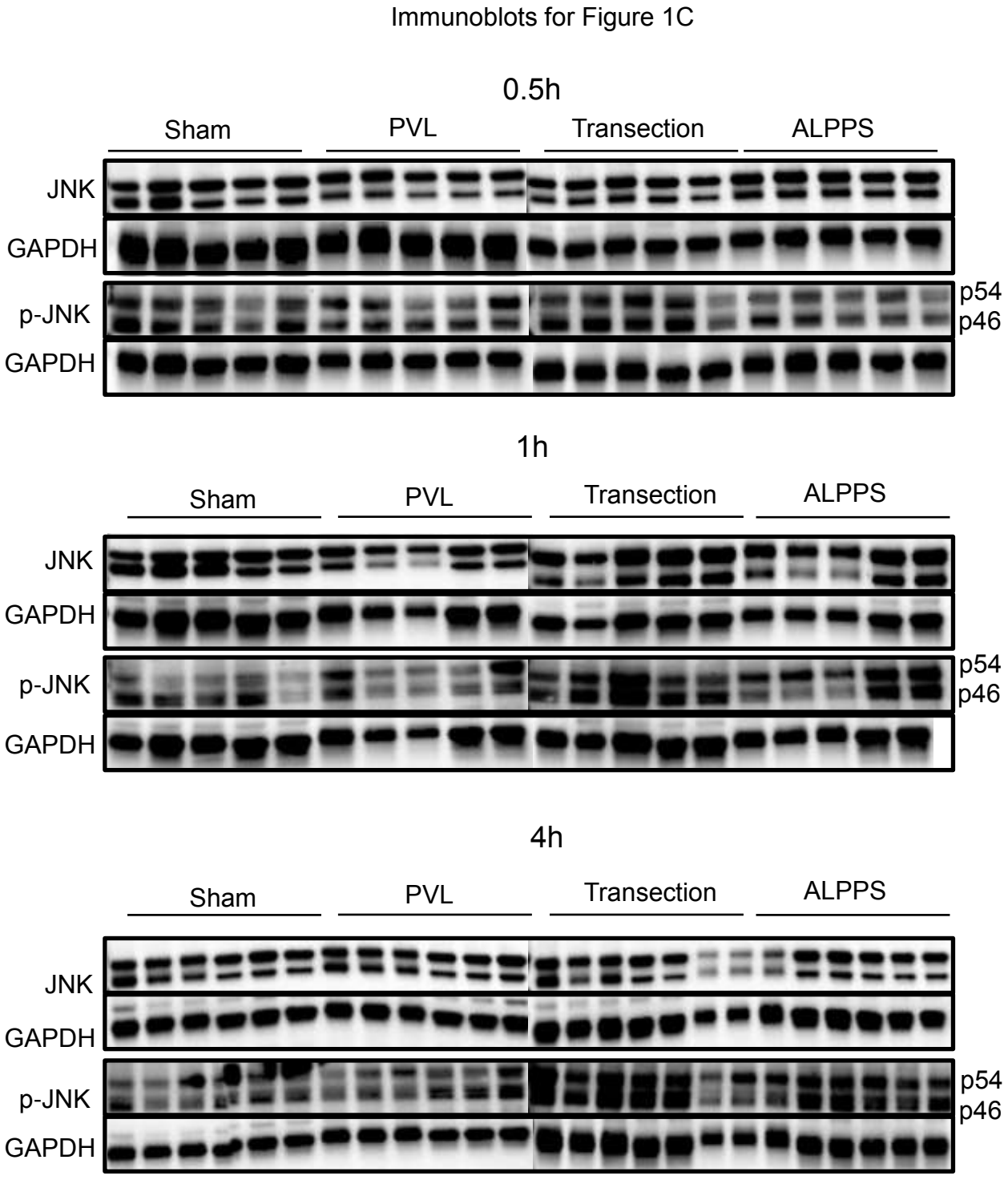

Immunoblots for Figure 1C

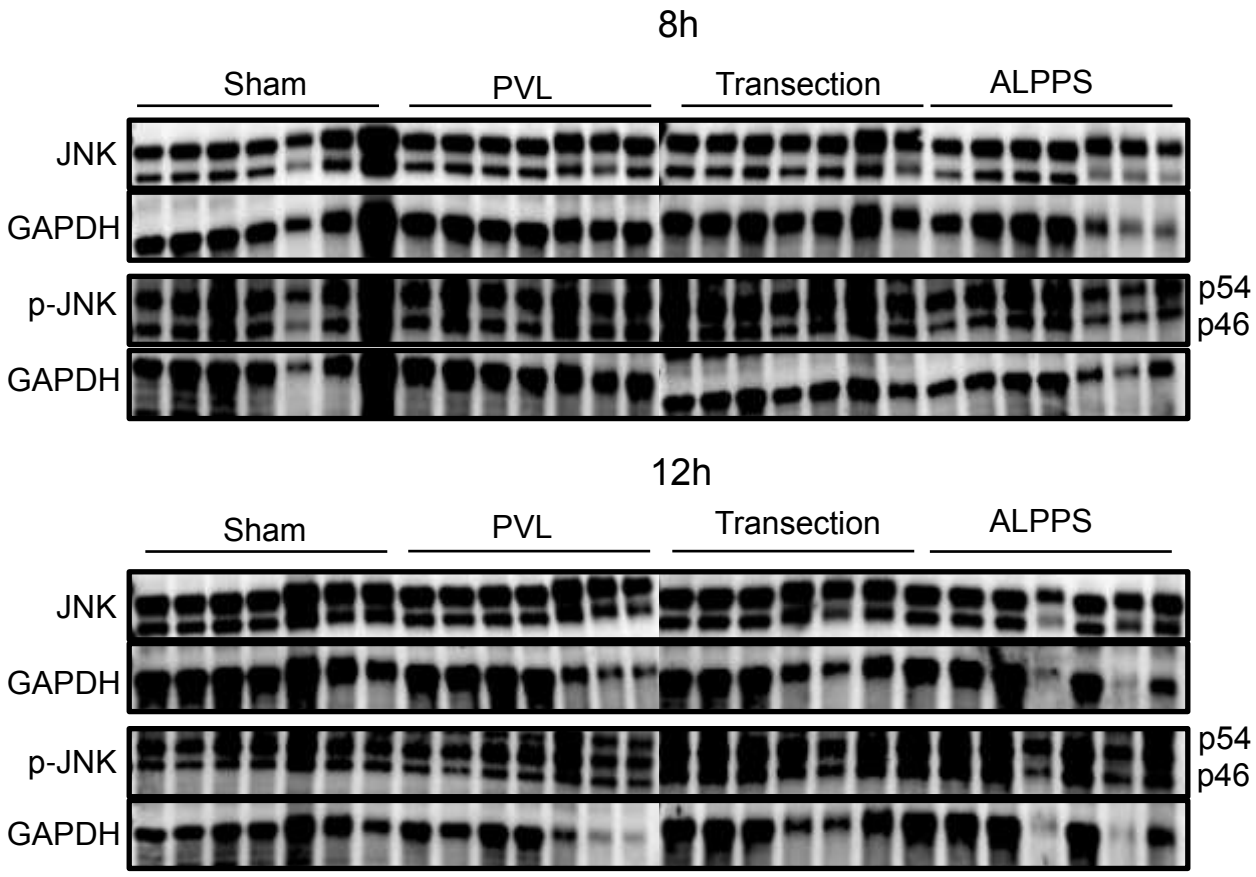

Immunoblots for Figure 2B, S3

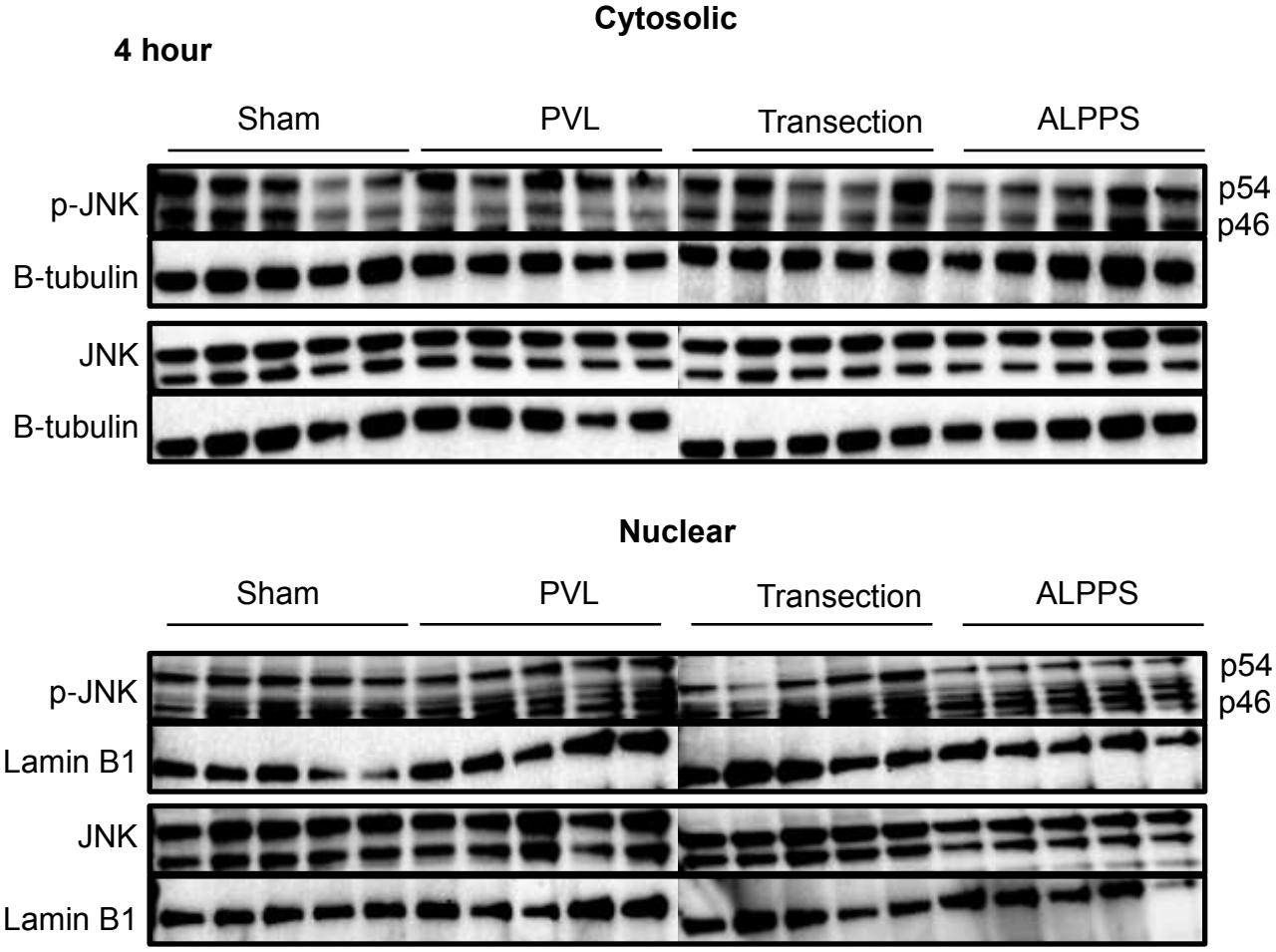

Immunoblots for Figure 2B, S3

24 hour

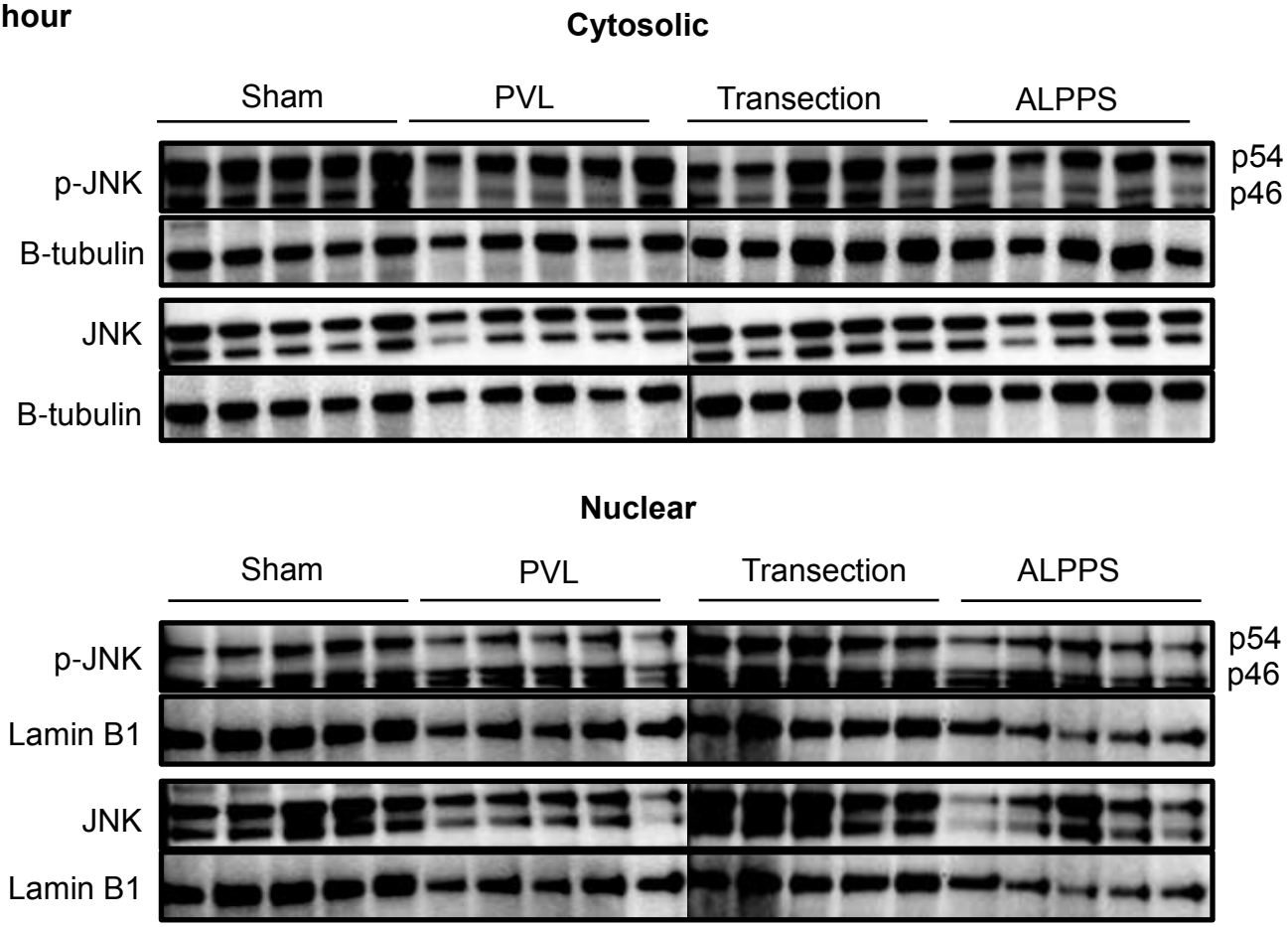

Immunoblots for Figure 2B, S3

4 hour

Cytosolic

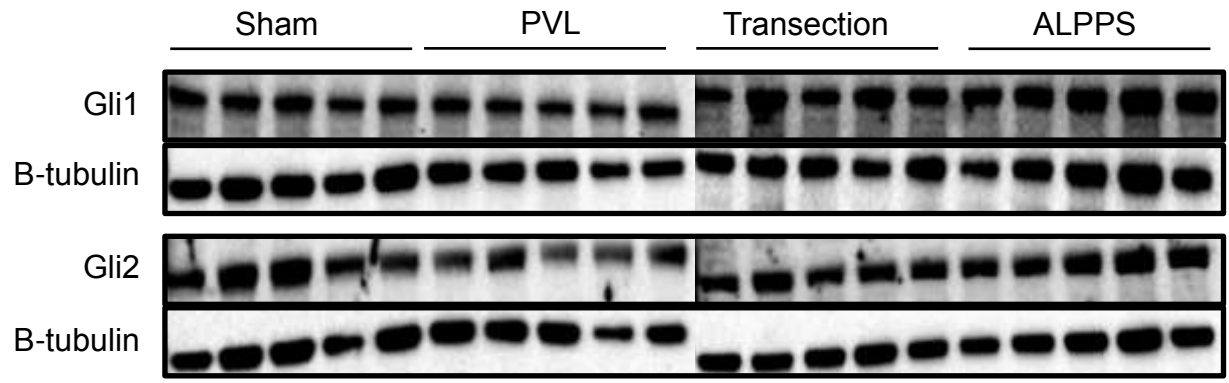

Nuclear

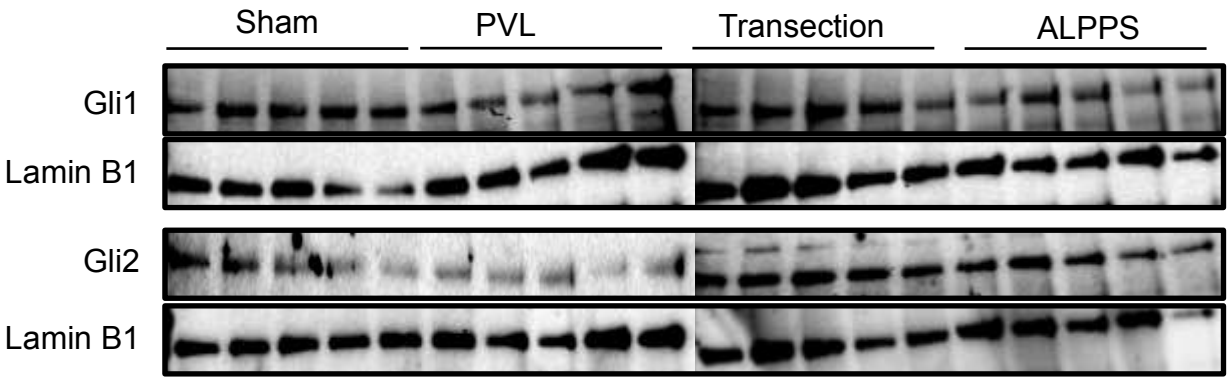

Cytosolic

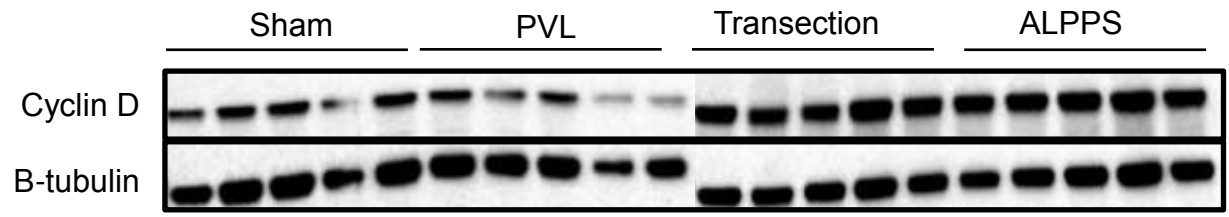

Nuclear

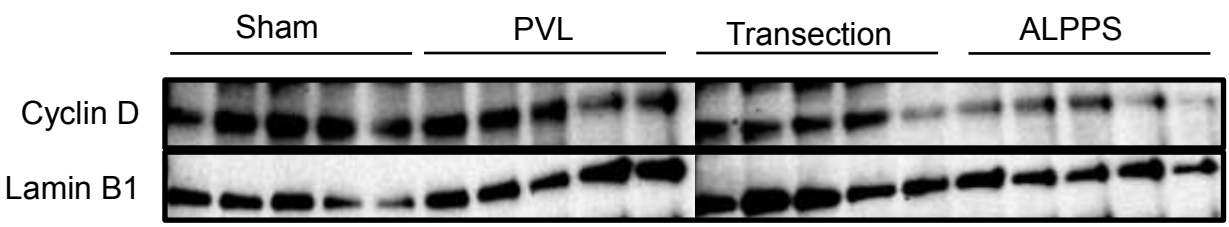

Immunoblots for Figure 2B, S3

24 hour

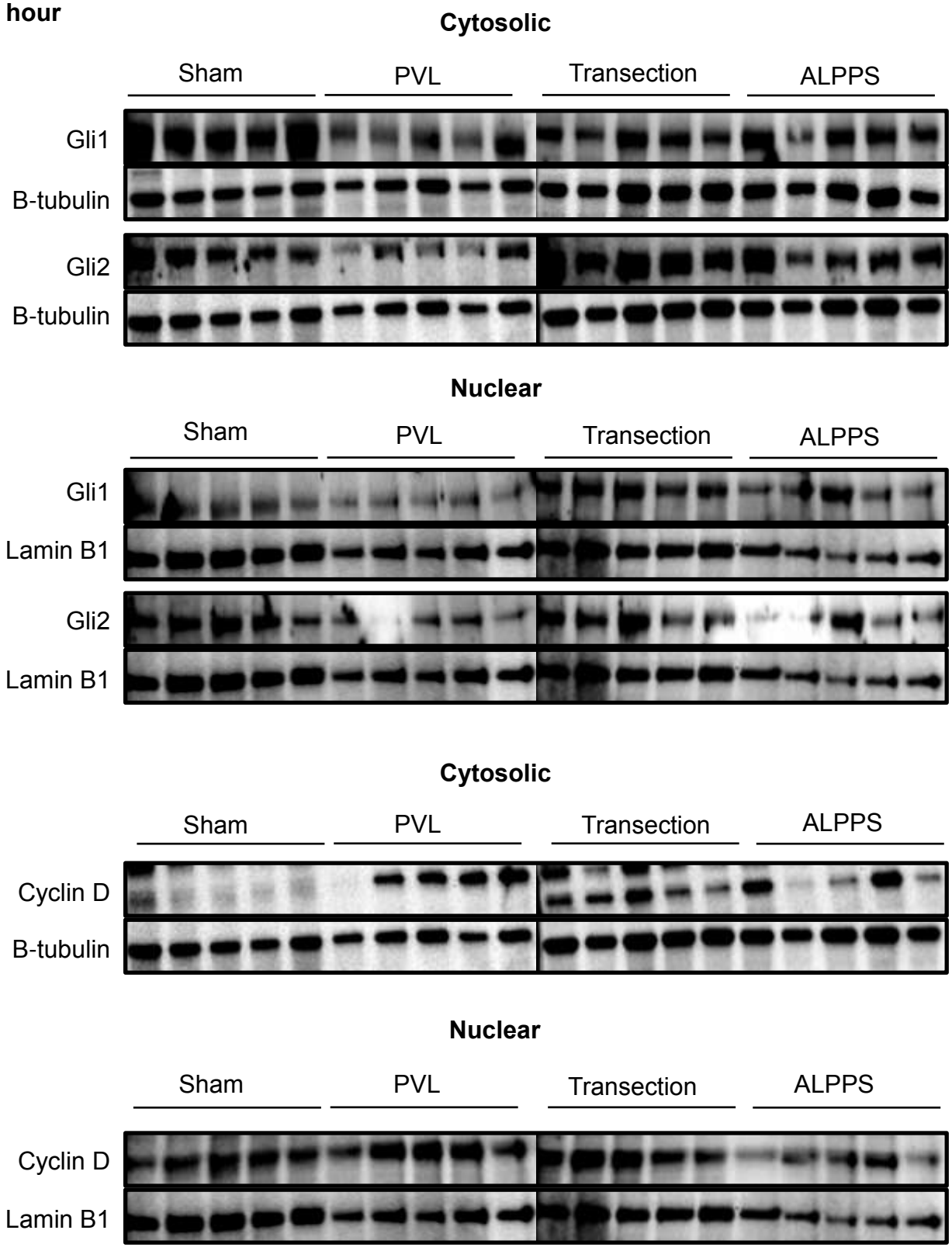

Immunoblots for Figure 3A, S5

4 hour

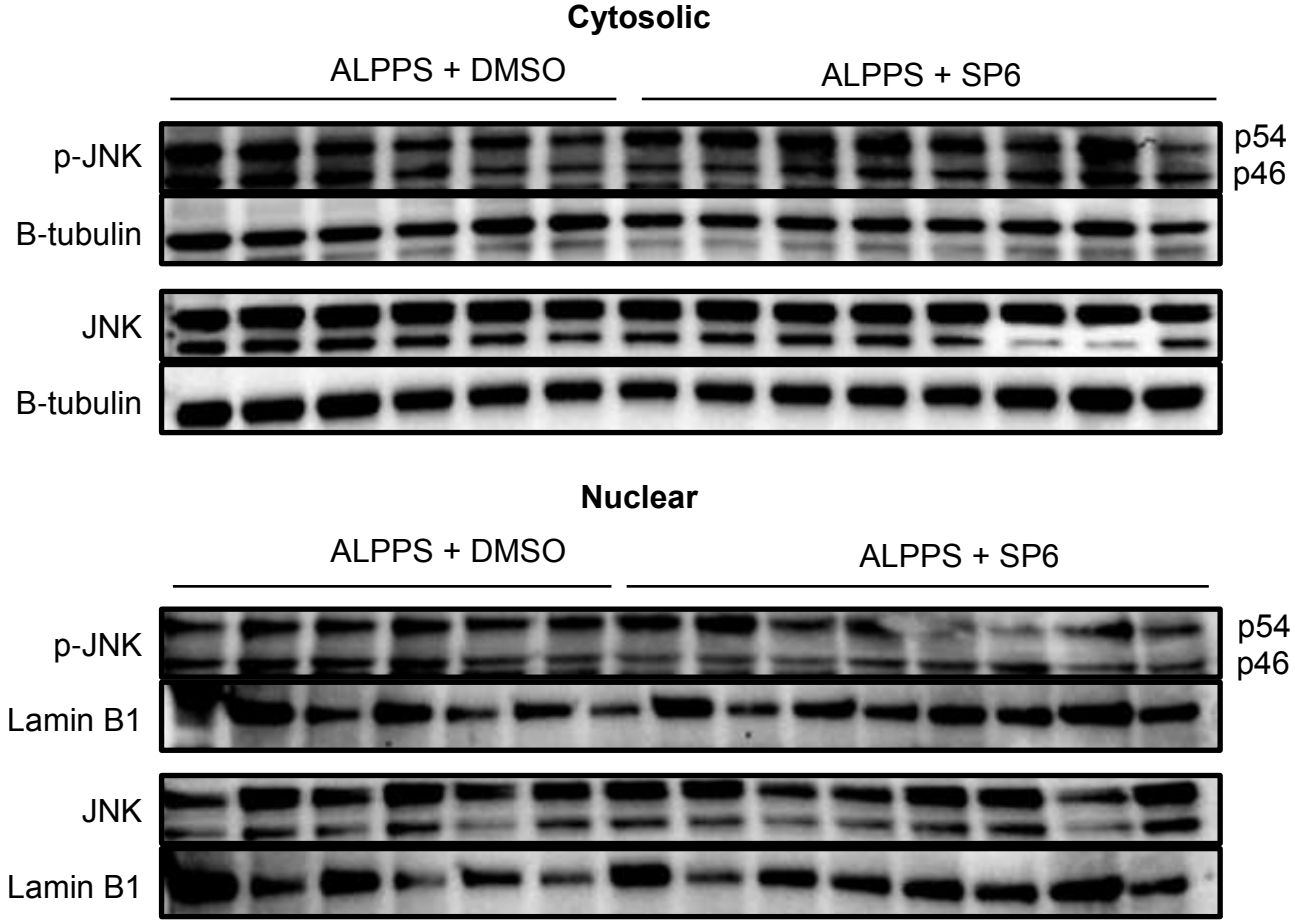

Immunoblots for Figure 3A, S5

24 hour

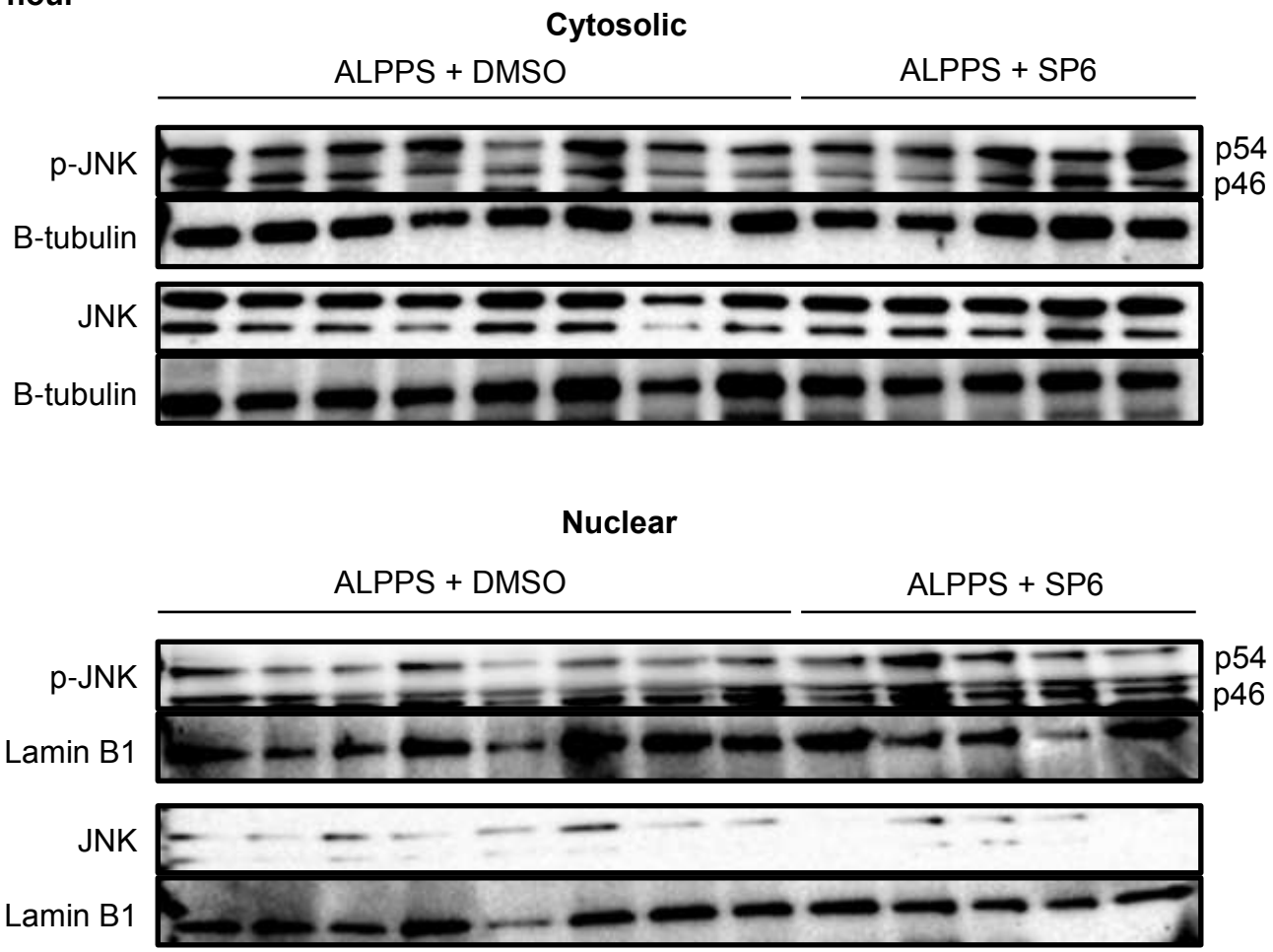

4 hour

Immunoblots for Figure 4A

Whole Tissue

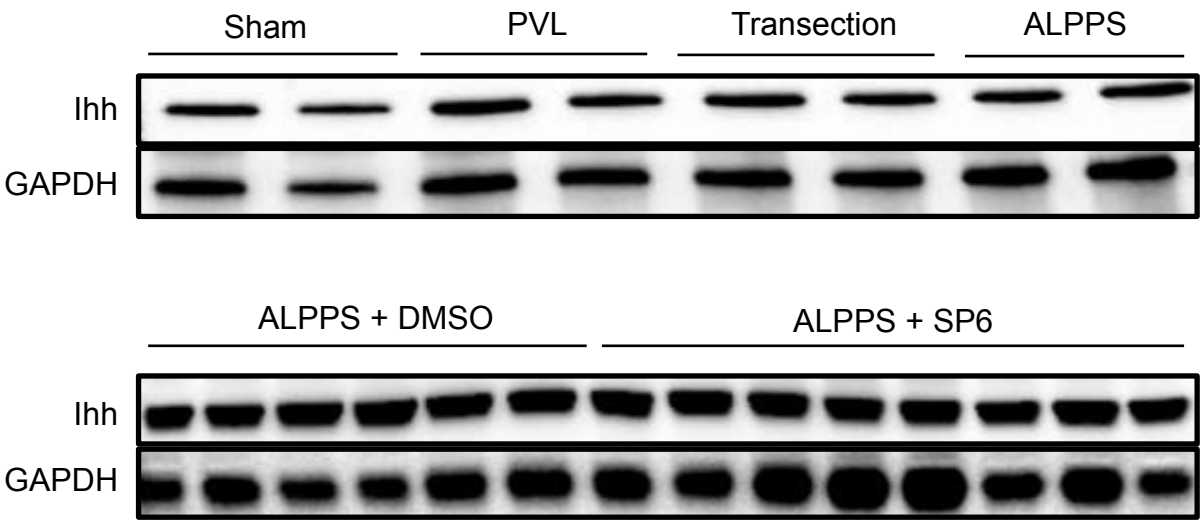

24 hour

Whole Tissue

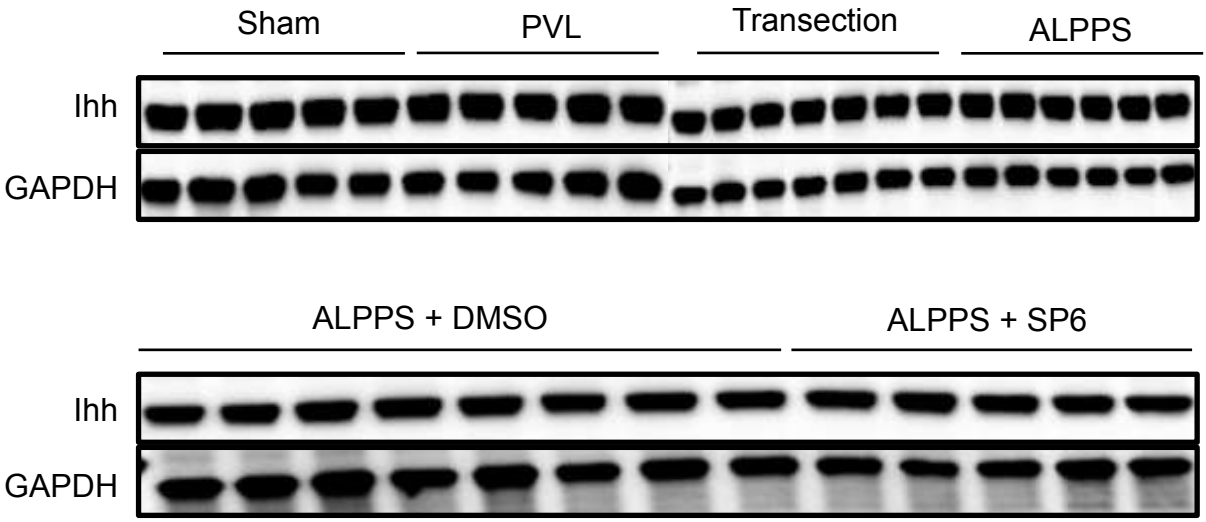

Immunoblots for Figure 4D, S8

4 hour

Cytosolic

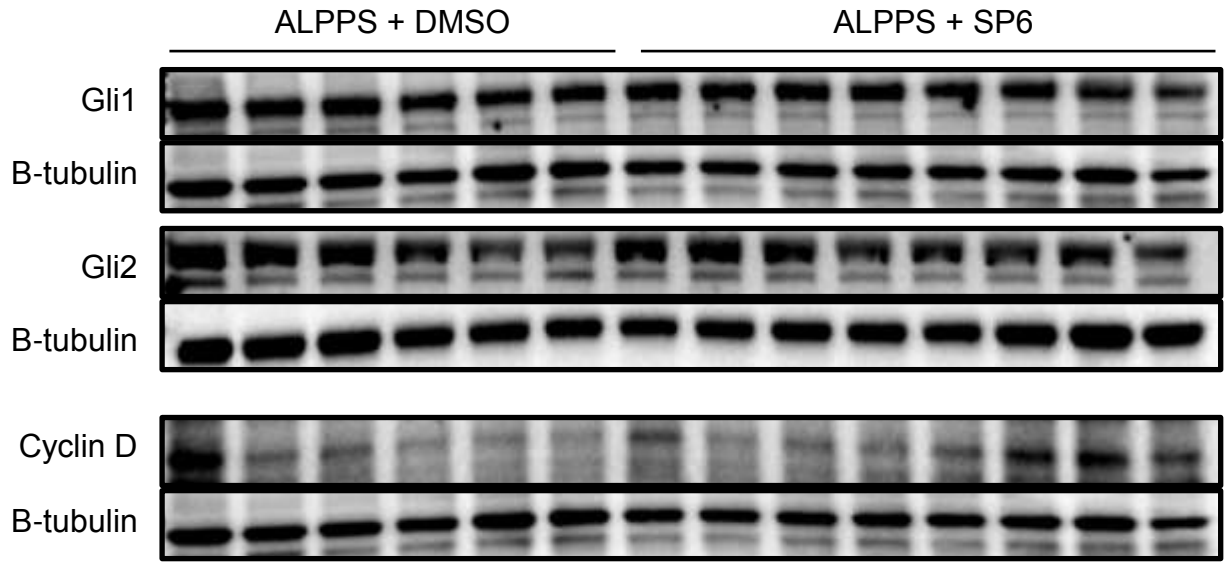

Nuclear

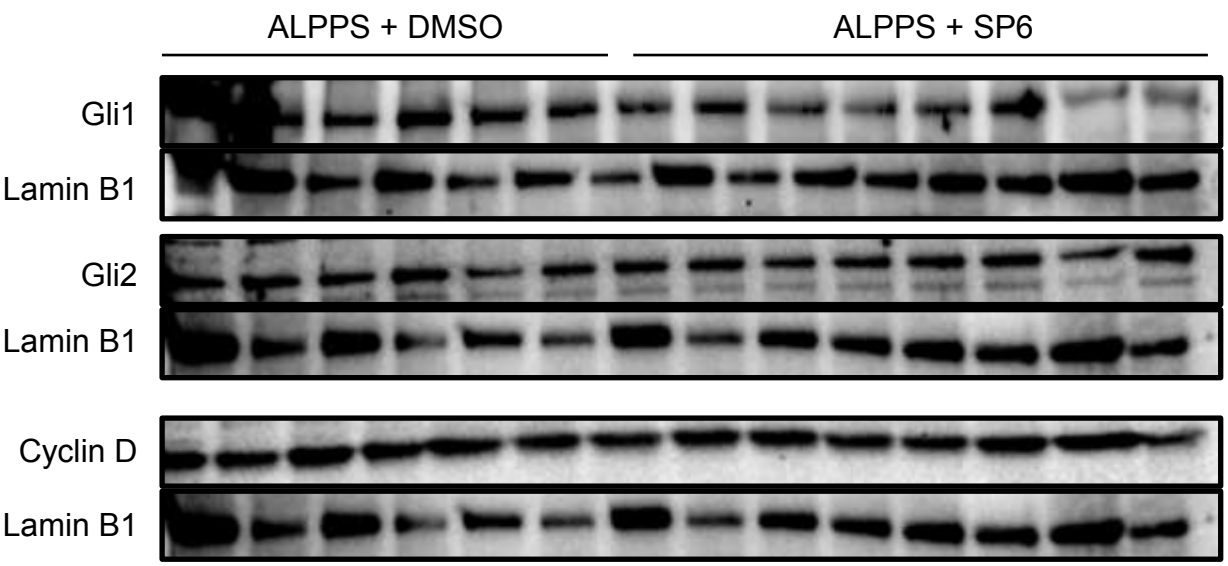

Immunoblots for Figure 4D, S8

24 hour

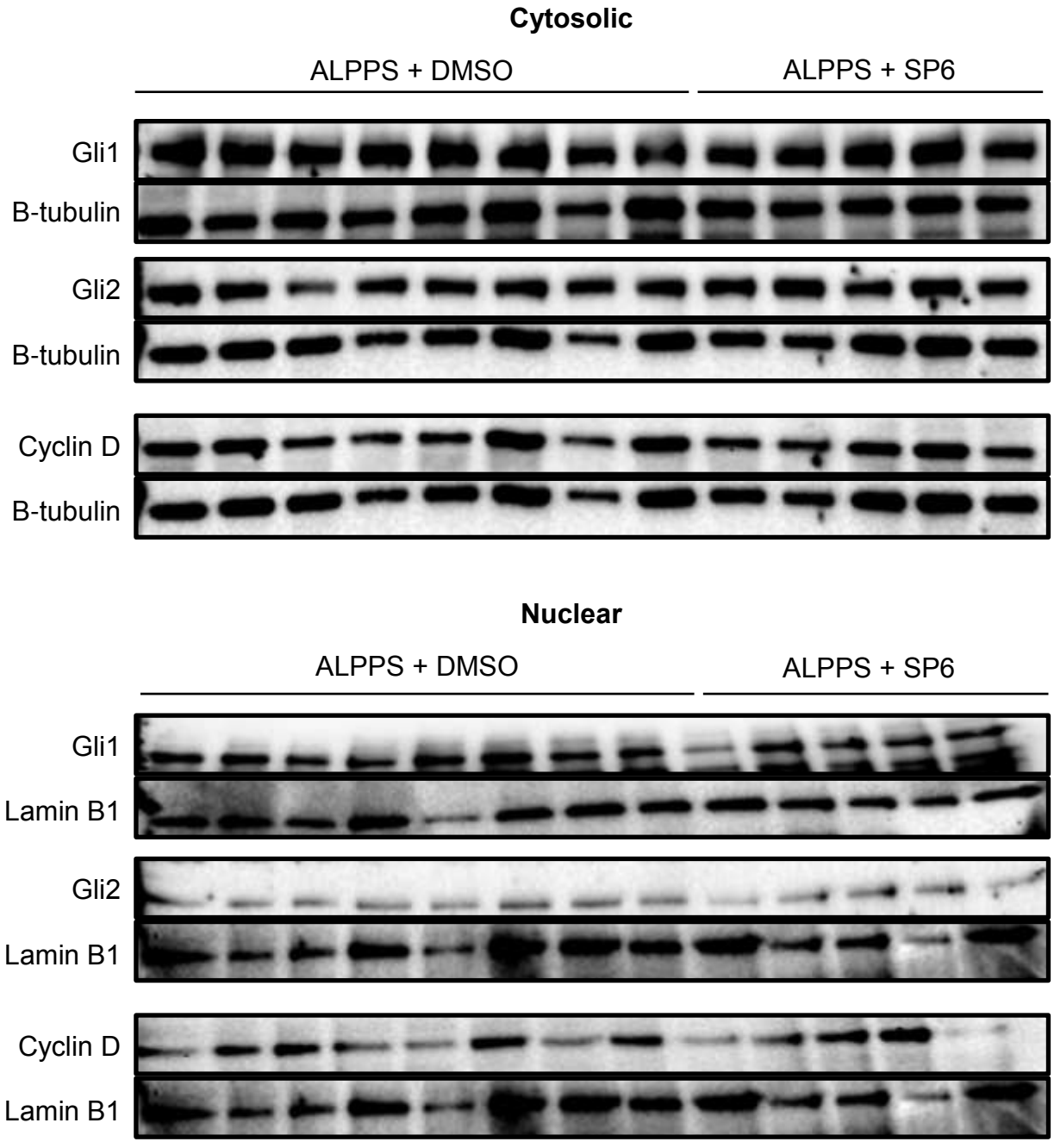

Immunoblots for Figure 6B, S13

4 hour

Cytosolic

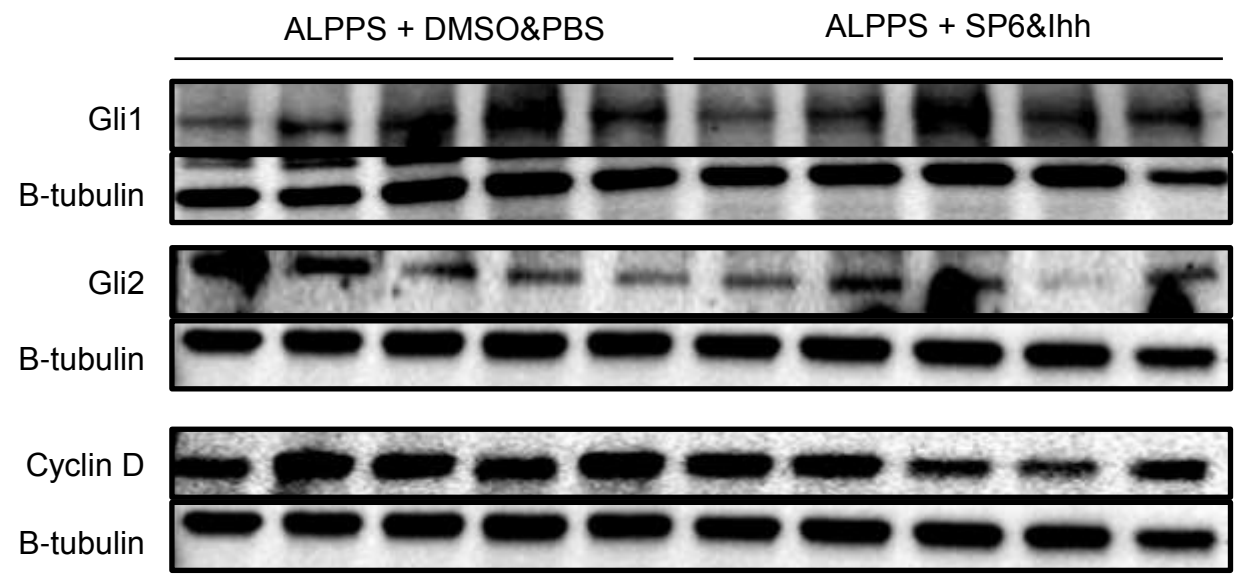

Nuclear

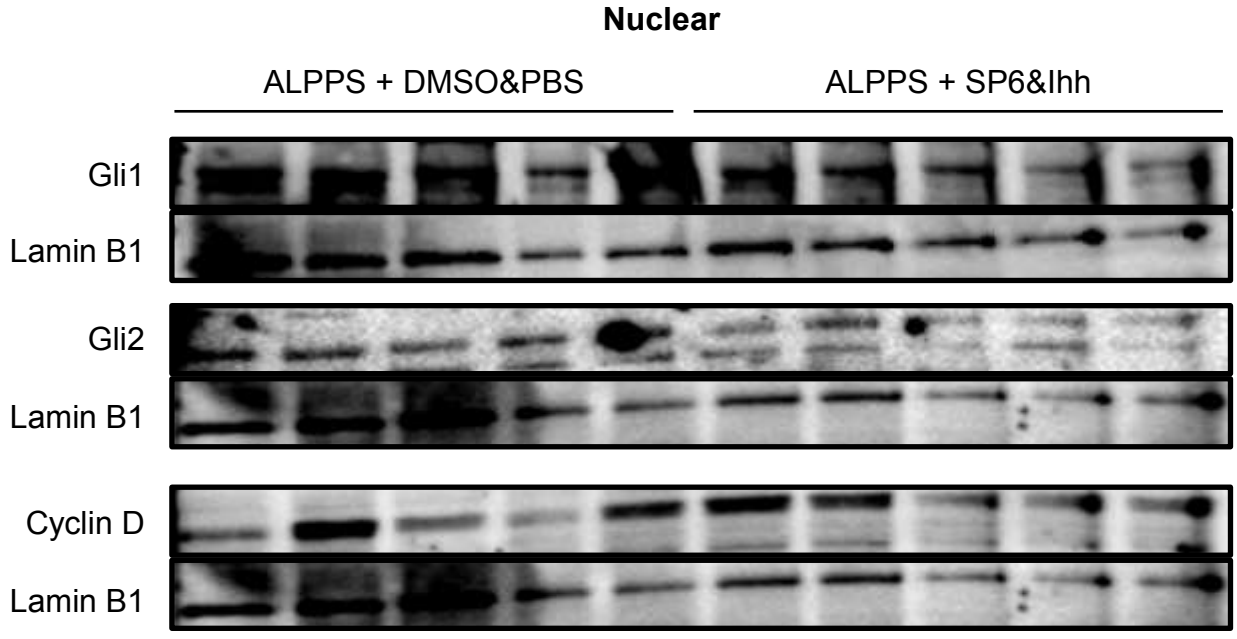

Immunoblots for Figure 6B, S13

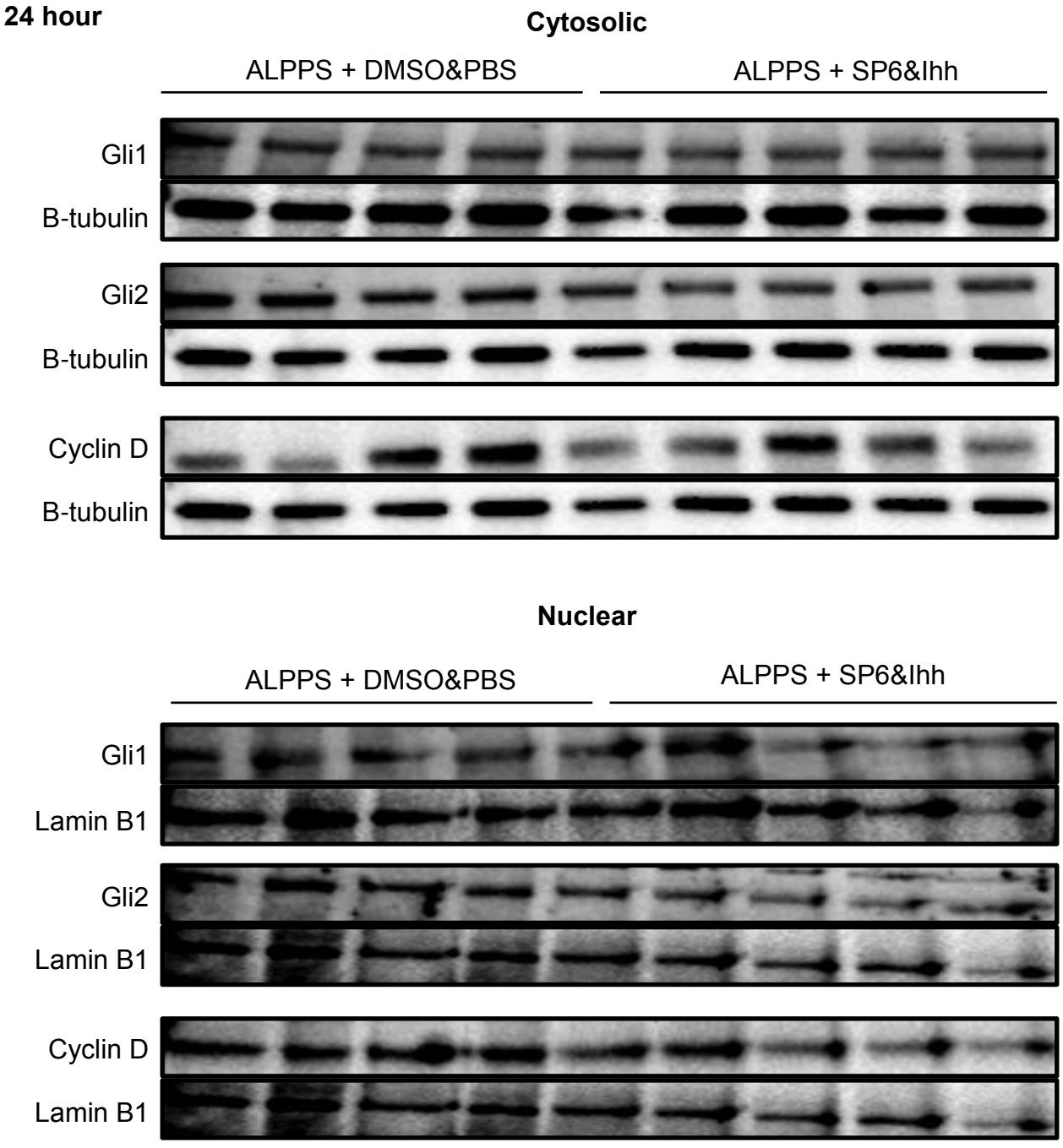

Immunoblots for Figure 6E, S14

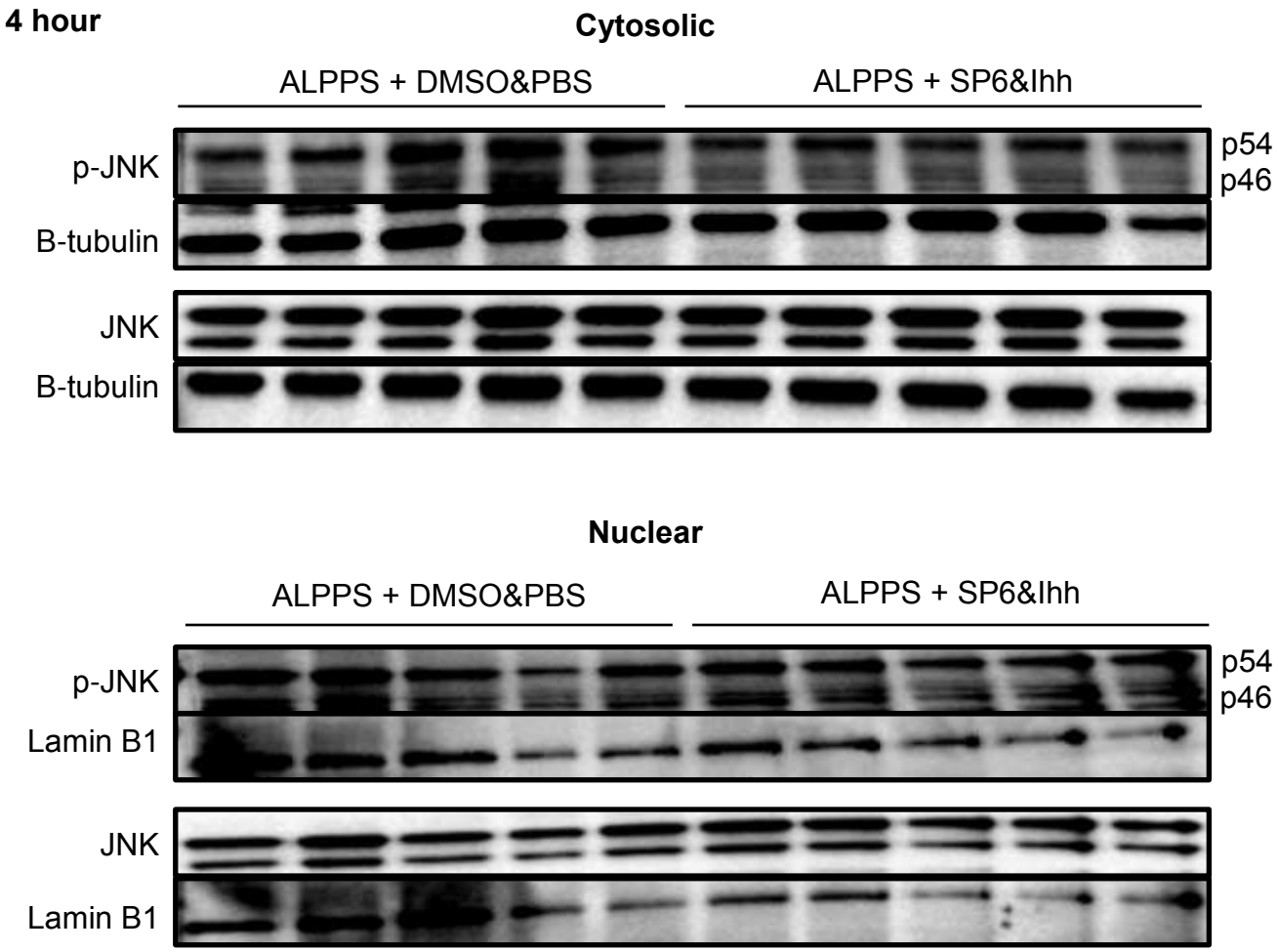

Immunoblots for Figure 6E, S14

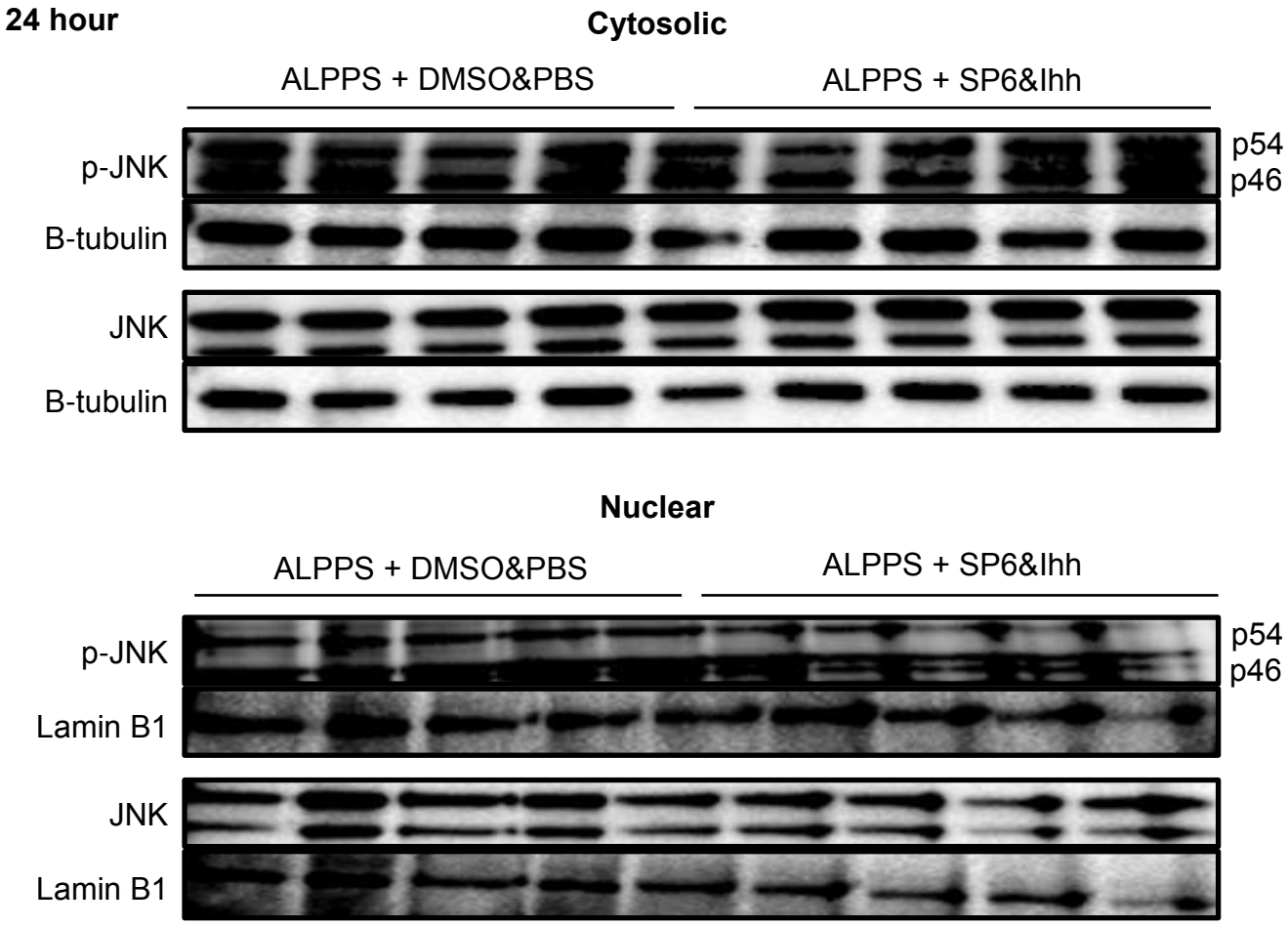

Figure 1

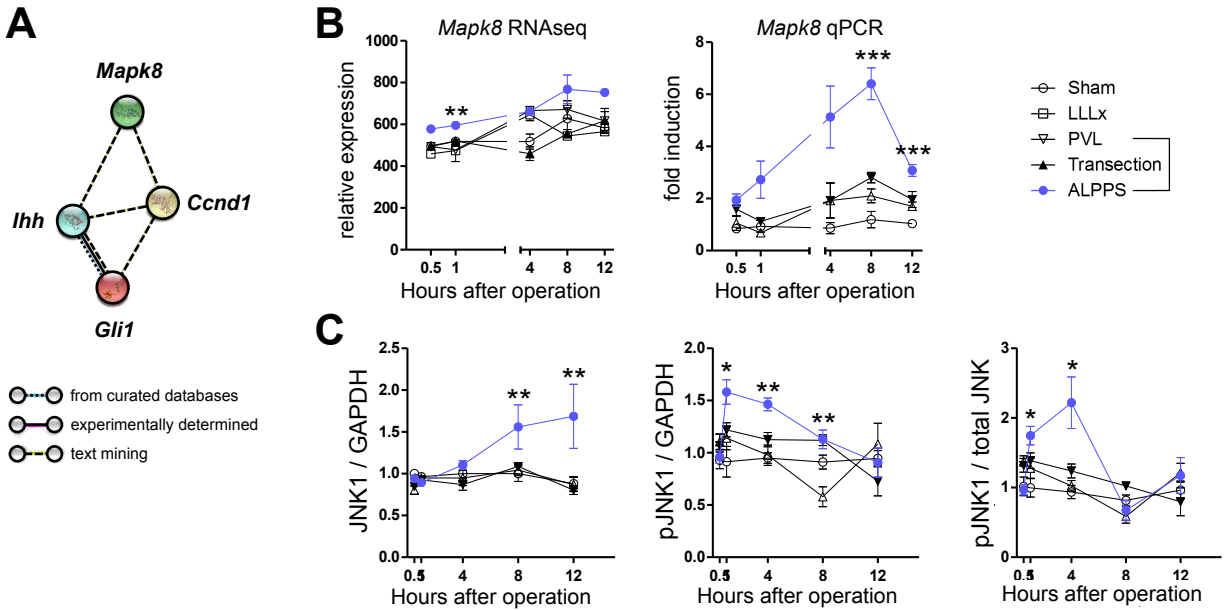
A
Mapk8
Ihh
Ccnd1
Gli1
from curated databases
experimentally determined
text mining
B
Mapk8 RNAseq
relative expression
1000
800
600
400
200
0
**
0.5
1
4
8
12
Hours after operation
Mapk8 qPCR
fold induction
8
6
4
2
0
***
***
0.5
1
4
8
12
Hours after operation
Sham
LLLx
PVL
Transection
ALPPS
C
JNK1 / GAPDH
2.5
2.0
1.5
1.0
0.5
0.0
**
**
0.5
4
8
12
Hours after operation
pJNK1 / GAPDH
2.0
1.5
1.0
0.5
0.0
*
**
**
0.5
4
8
12
Hours after operation
pJNK1 / total JNK
3
2
1
0
*
*
0.5
4
8
12
Hours after operation

Figure 2

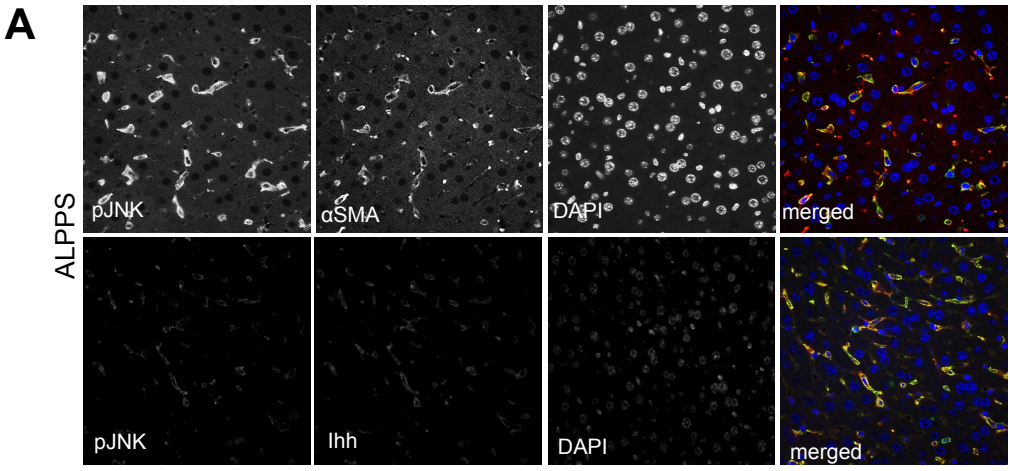
A
ALPPS
pJNK
αSMA
DAPI
merged
pJNK
Ihh
DAPI
merged

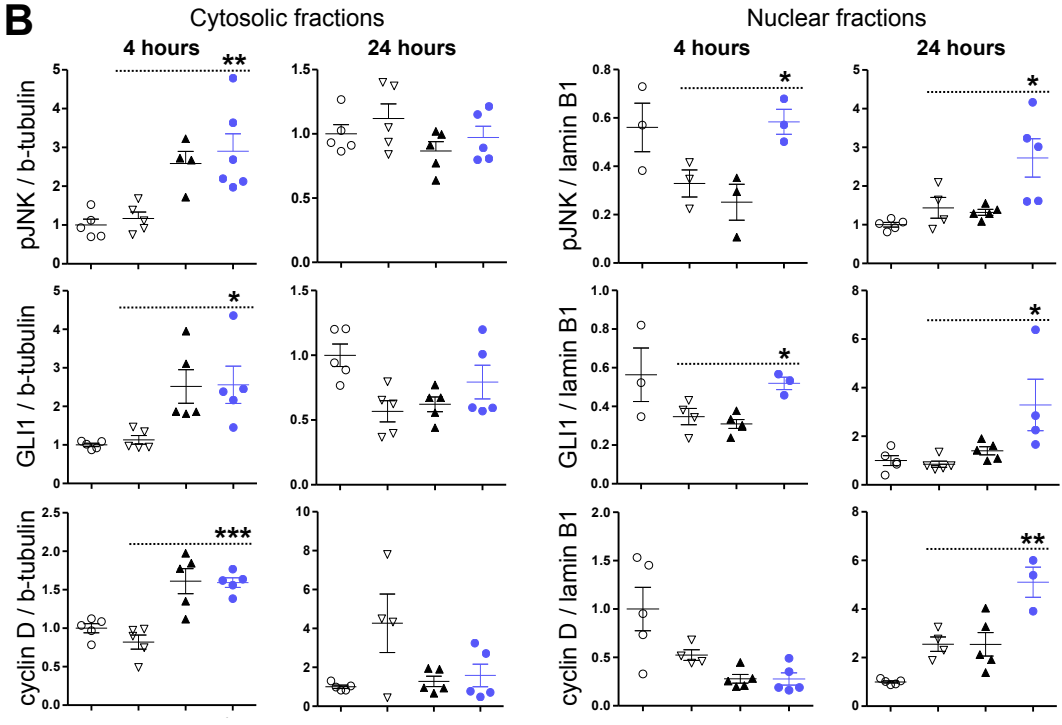
B
Cytosolic fractions
Nuclear fractions
4 hours
24 hours
4 hours
24 hours
pJNK / b-tubulin
GLI1 / b-tubulin
cyclin D / b-tubulin
pJNK / lamin B1
GLI1 / lamin B1
cyclin D / lamin B1

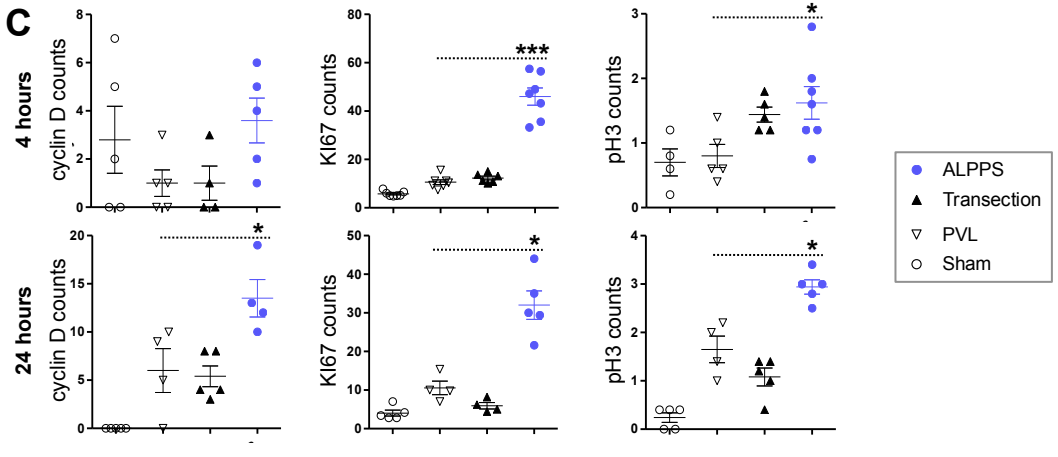
C
4 hours
24 hours
cyclin D counts
KI67 counts
pH3 counts
ALPPS
Transection
PVL
Sham

Figure 3

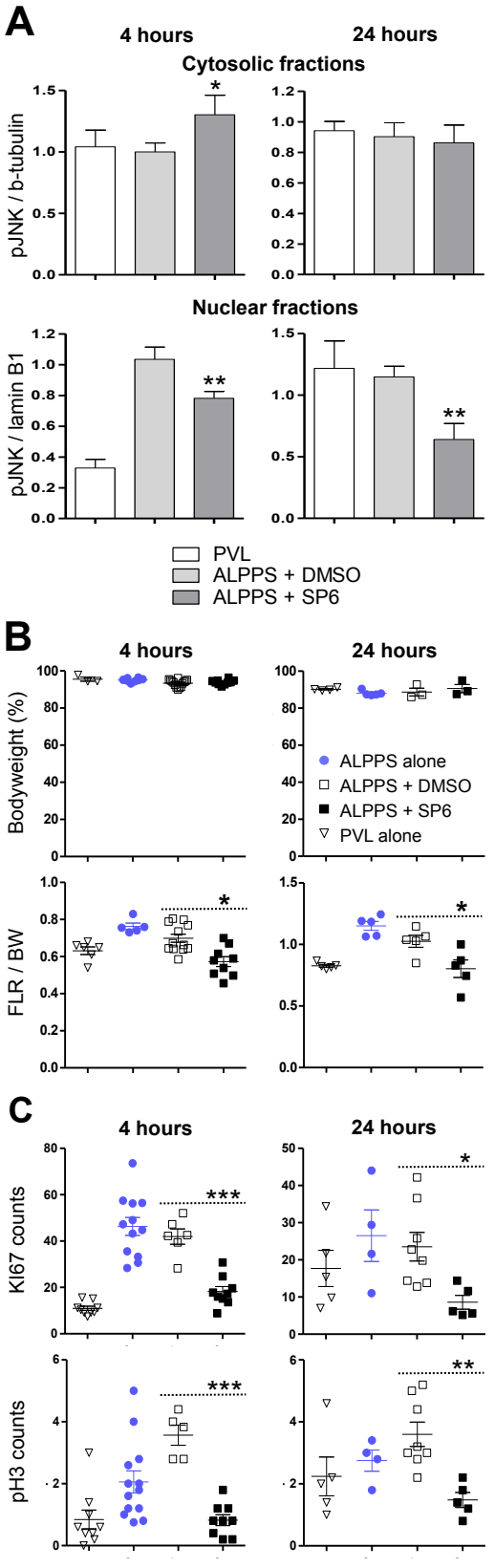
A
4 hours
24 hours
Cytosolic fractions
pJNK / b-tubulin
Nuclear fractions
pJNK / lamin B1
PVL
ALPPS + DMSO
ALPPS + SP6
B
4 hours
24 hours
Bodyweight (%)
ALPPS alone
ALPPS + DMSO
ALPPS + SP6
PVL alone
FLR / BW
C
4 hours
24 hours
KI67 counts
pH3 counts

Figure 4

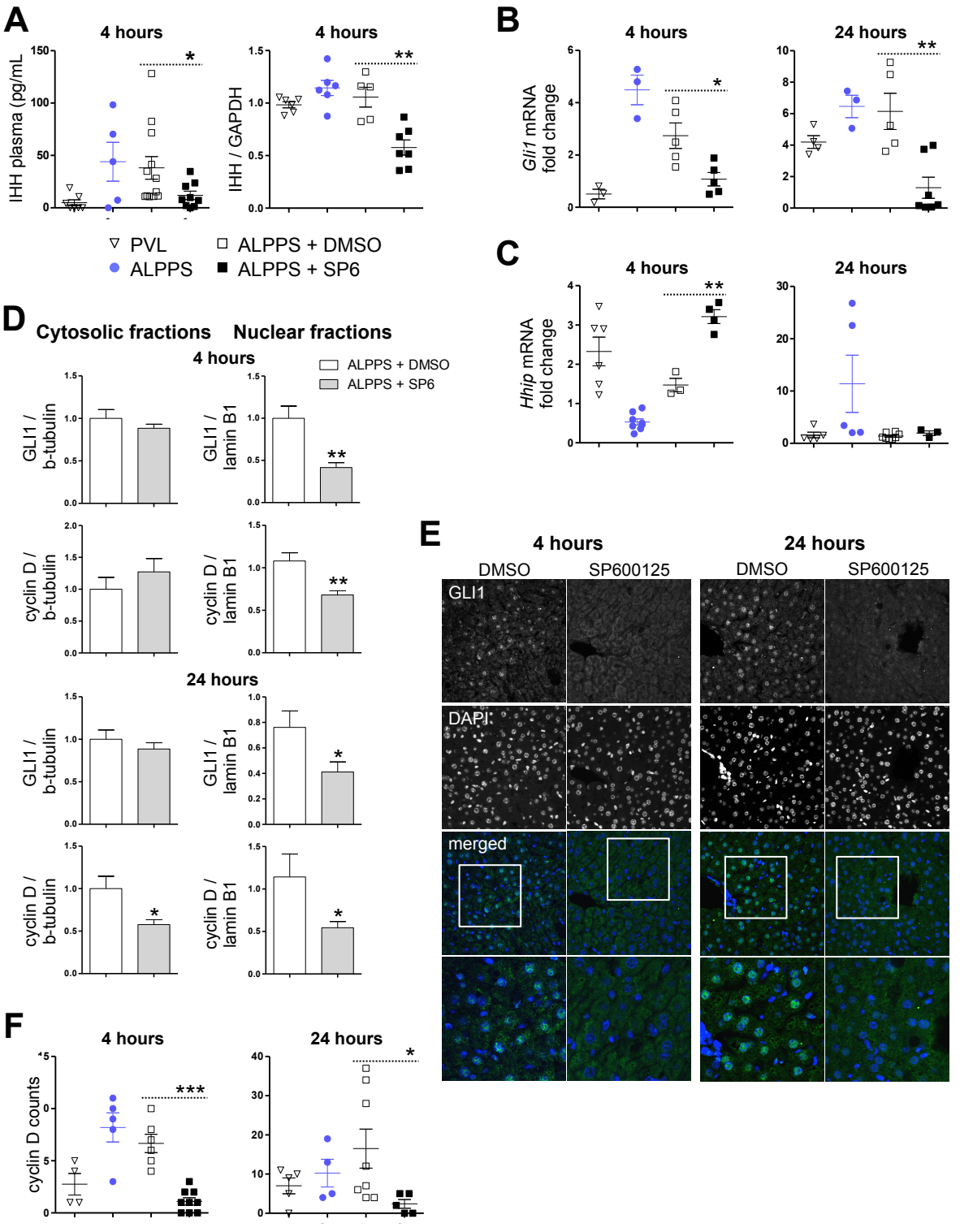
A
4 hours
IHH plasma (pg/mL)
4 hours
IHH / GAPDH
PVL
ALPPS
ALPPS + DMSO
ALPPS + SP6
B
4 hours
24 hours
Gli1 mRNA fold change
C
4 hours
24 hours
Hhip mRNA fold change
D
Cytosolic fractions
Nuclear fractions
4 hours
ALPPS + DMSO
ALPPS + SP6
GLI1 / b-tubulin
GLI1 / lamin B1
cyclin D / b-tubulin
cyclin D / lamin B1
24 hours
E
4 hours
24 hours
DMSO
SP600125
GLI1
DAPI
merged
F
4 hours
24 hours
cyclin D counts

Figure 5

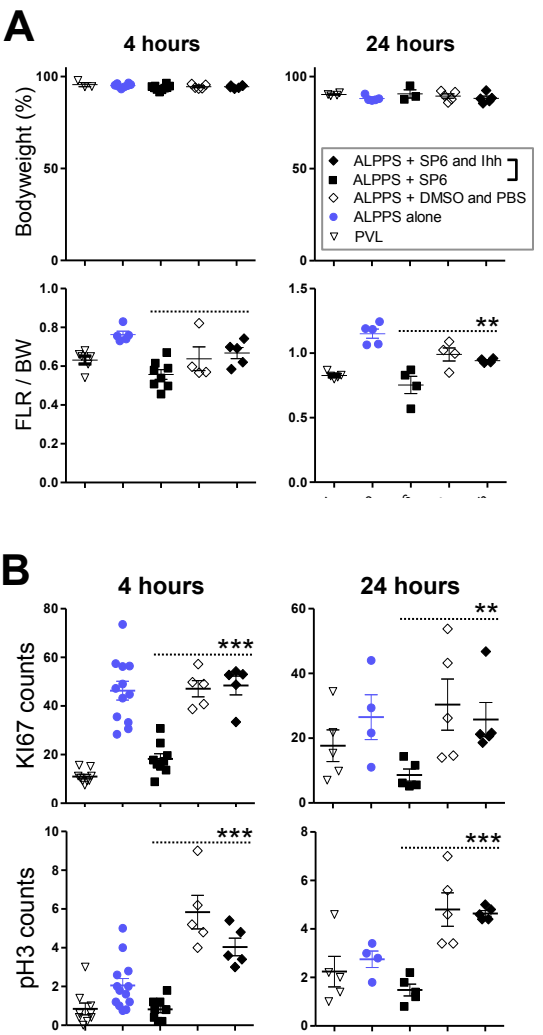
A
4 hours
24 hours
Bodyweight (%)
FLR / BW
ALPPS + SP6 and Ihh
ALPPS + SP6
ALPPS + DMSO and PBS
ALPPS alone
PVL
**
B
4 hours
24 hours
KI67 counts
pH3 counts
***
**
***

Figure 6

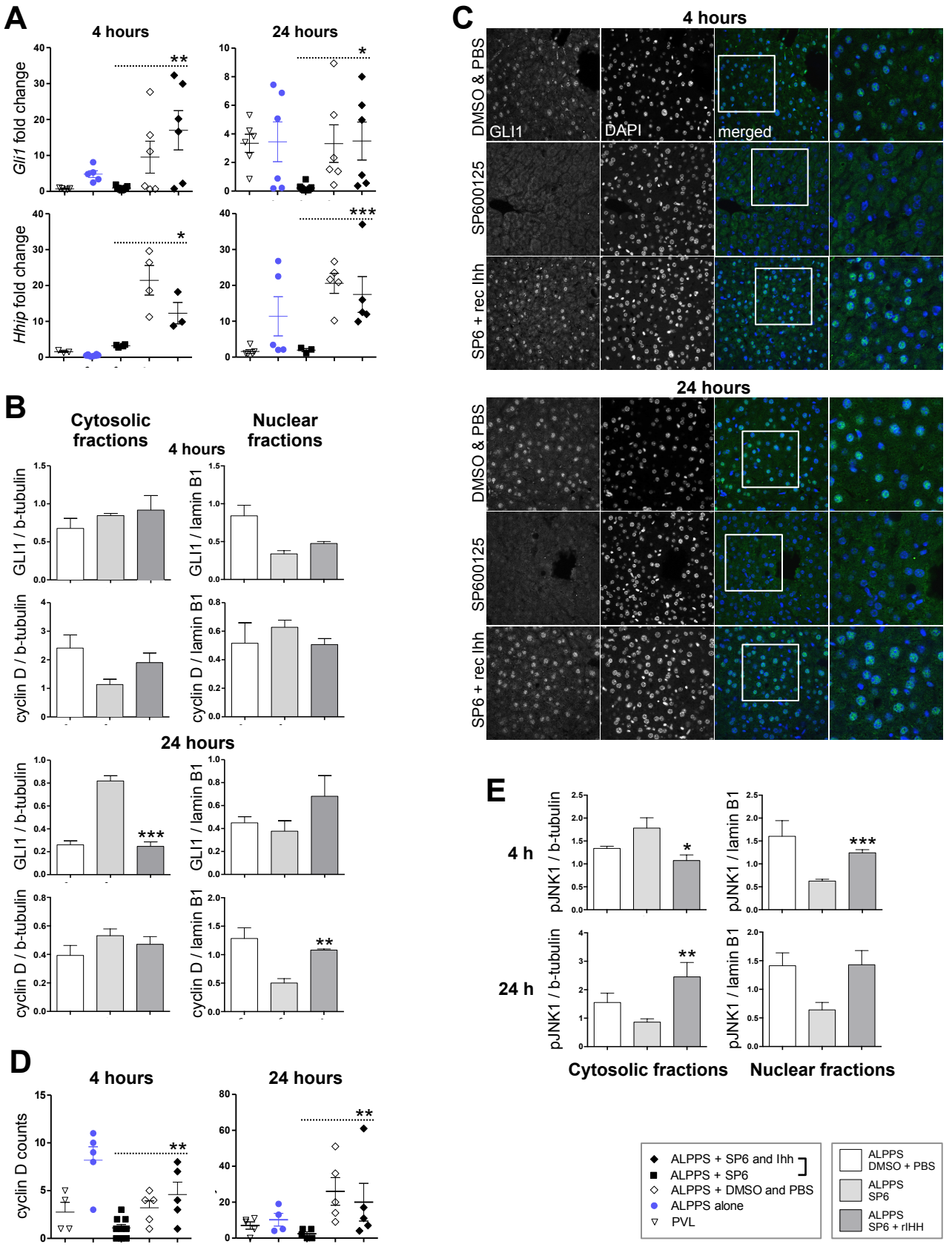
A
4 hours
24 hours
Gli1 fold change
Hhip fold change
B
Cytosolic fractions
Nuclear fractions
4 hours
24 hours
GLI1 / b-tubulin
cyclin D / b-tubulin
GLI1 / lamin B1
cyclin D / lamin B1
C
4 hours
24 hours
DMSO & PBS
SP600125
SP6 + rec Ihh
GLI1
DAPI
merged
D
cyclin D counts
E
4 h
24 h
pJNK1 / b-tubulin
pJNK1 / lamin B1
Cytosolic fractions
Nuclear fractions
ALPPS + SP6 and Ihh
ALPPS + SP6
ALPPS + DMSO and PBS
ALPPS alone
PVL
ALPPS DMSO + PBS
ALPPS SP6
ALPPS SP6 + rIHH